IN-37
72743
93P.

DOE/NASA/0343-1
NASA CR-179570
MTI 86TR33

EHD Analysis of and Experiments on Pumping Leningrader Seals

M.W. Eusepi and J.A. Walowit
Mechanical Technology Incorporated

June 1986

Prepared for
NATIONAL AERONAUTICS AND SPACE ADMINISTRATION
Lewis Research Center
Under Contract DEN 3-343

for
U.S. DEPARTMENT OF ENERGY
Conservation and Renewable Energy
Office of Vehicle and Engine R&D

DISCLAIMER

Printed in the United States of America

Available from
National Technical Information Service
U.S. Department of Commerce
5285 Port Royal Road
Springfield, VA 22161

NTIS price codes[1]
Printed copy: A05
Microfiche copy: A01

[1]Codes are used for pricing all publications. The code is determined by the number of pages in the publication. Information pertaining to the pricing codes can be found in the current issues of the following publications, which are generally available in most libraries: *Energy Research Abstracts (ERA); Government Reports Announcements* and Index (*GRA* and I); *Scientific and Technical Abstract Reports (STAR);* and publication, NTIS-PR-360 available from NTIS at the above address.

DOE/NASA/0343-1
NASA CR-179570
MTI 86TR33

EHD Analysis of and Experiments on Pumping Leningrader Seals

M.W. Eusepi and J.A. Walowit
Mechanical Technology Incorporated
Latham, New York 12110

June 1986

Prepared for
National Aeronautics and Space Administration
Lewis Research Center
Cleveland, Ohio 44135
Under Contract DEN 3-343

for
U.S. DEPARTMENT OF ENERGY
Conservation and Renewable Energy
Office of Vehicle and Engine R&D
Washington, D.C. 20545
Under Interagency Agreement DE-AI01-85CE50112

TABLE OF CONTENTS

TABLE OF CONTENTS (Continued)

NOMENCLATURE

C = Constant

D = Flexural rigidity $Et^3/12(1 - \nu^2)$

E = Elastic modulus

F = Shear force at $x = 0$

h = Film thickness

h_o = Value of h where $(dp/dx) = 0$

$\bar{h}$ = $h/(\delta_s + \delta_o)$

$\hat{h}$ = $(h - h_o)/h_o$

i = $\sqrt{-1}$

ℓ_e = Diffusion length, $\sqrt{Rt}/[12(1-\nu^2)]^{1/4}$

L_r = x extent of seal lift-off

$\bar{L}_r$ = $-(L_r/\ell_e)$

p = Pressure

p_g = Sealed gas pressure

p_s = $Et\delta_s/R^2$

p_o = Oil pressure; also p at start of film

$\bar{p}$ = $(p - p_o)/(p_s + p_g - p_o)$

$$\hat{p} = \frac{\delta_s}{h_o}\left[\left(\frac{p - p_g}{p_s}\right) - \left(1 + \frac{h_o}{\delta_s}\right)\right]$$

$\bar{p}_o = (p_g - p_o)/p_o$

R_s = Radius of shaft

R_i = Inner radius of seal

R = Effective radius, $R_i + (t/2)$

t = Thickness of seal wall

U = Shaft linear velocity

x = Horizontal coordinate (in direction of U)

x_m = Location of maximum pressure

$\bar{x} = -(x/\ell_e)$

w = Displacement coordinate (normal to U)

$\bar{w} = -(w - \delta_o)/(\delta_s + \delta_o)$

$$\beta = \frac{6\mu U \ell_e \delta_s}{h_o^3 p_s} = \frac{6\mu U \ell_e R^2}{Et h_o^3}$$

$$\beta_1 = \frac{6\mu U \ell_e R^2}{Et (\delta_o \delta_s)}$$

β_a = Approximate value of β

δ = Interference (positive or negative)

δ_o = Interference due to $(p_g - p_o)$, $R^2(p_g - p_o)/Et$

δ_s = Interference due to shaft

δ_r = Interference due to expansion ring

$\bar{\delta}_r$ = $(\delta_r - \delta_s)/(\delta_o + \delta_s)$

μ = Viscosity

ν = Poissons ratio

Subscripts

s = shaft

r = ring

j = index

SUMMARY

An analysis has been developed to predict the performance of pumping Leningrader reciprocating rod seals when the inlet (gas) side of the seal bore is formed by an expansion ring rather than by machining. The prediction of seal performance is based on the use of charts which provide necessary design parameters without the need for computerized calculations. A numerical example has been included to demonstrate the use of the design charts. Potential means for controlling and optimizing both performance and life capability is also provided.

An experimental study was also conducted as part of the overall program in order to evaluate pumping Leningrader seals constructed in accordance with the analysis. Several seal materials, ranging in elastic modulus from 1.59×10^3 MPa for filled PTFE to 4.58×10^3 MPa for poly(amide-imide) were tested. For the limited number and durational tests conducted, the experiments showed that the ring expanded inlet type seal has the ability to provide desired levels of sealing. Additionally, it was shown that the lower modulus materials are more easily fabricated into seals and provide better sealing capability.

1.0 INTRODUCTION

The Pumping Leningrader Seal has been used successfully as a rod seal for Automotive Stirling Engine (ASE) applications. It is used for sealing the working fluid (hydrogen) at pressures to 15 MPa against an ambient lubricating oil. An analysis was performed to obtain quantitative predictions of the mechanism by which the seal operates and to suggest potential means of controlling and optimizing seal performance and life.

The analytical techniques divide the seal into three regions: an inlet zone, a contact zone, and an exit zone. The film thickness is largely determined by inlet zone behavior, and the sensitivity of the film thickness and flow rate to inlet zone geometry was evaluated. The inlet type investigated was one where an inlet zone is induced with an expansion ring. Complete solutions have been obtained for several ring geometries by matching solutions in the three zones. The analysis predicts very strong sensitivity near the inlet that will be wear sensitive. The ring-induced inlet is predicted to provide a larger film and lower sensitivity to wear than does the premachined inlet currently incorporated in pumping ring seals.

Experiments were performed on selected seal geometries for several seal materials ranging in elastic modulus from 1.59×10^3 MPa for a filled PTFE to 4.58×10^3 MPa for poly(amide-imide). Two sets of tests were performed on each seal. One test set was conducted with the test seals flooded with oil on what would normally be the side exposed to the high-pressure gas. The second test set was performed under normal seal conditions with high-pressure gas on one side of the seal and ambient pressure oil on the opposite side.

The flooded tests demonstrated the oil pumping capability of the experimental seals, a performance parameter readily calculated. The test conducted under normal seal operating conditions was used to demonstrate the gas sealing capability of the expanding ring inlet PL seal design.

This report covers the PL seal analysis including a numerical design example, experimental results of several flooded and gas bearing tests, and a discussion of results.

2.0 EHD ANALYSIS OF HYDRODYNAMIC PUMPING RING

2.1 The Mathematical Model

A schematic of the Leningrader seal is shown in Figure 2-1. The seal is mounted on the shaft with an interference fit and is separated from the oil side by a backup spring acting on the secondary static seal as well as by the force generated by the high-pressure gas. A converging inlet region provides pumping action during the forward stroke. During the backstroke, the seal rubs and wipes the oil away. Any oil that leaks toward the high-pressure gas will be pumped back toward the oil reservoir. The pressure p_o at the inlet to the seal corresponds to a case where the seal is isolated from p_g (by some secondary seal); if it is not, then $p_o = p_g$. While over the converging zone, the pressure will vary over most of the seal; past the initial point of contact, the pressures will be constant and equal to p_s, the hoop stresses induced by shaft interference.

The mathematical model of the seal is sketched in Figure 2-2. In part (a) the seal is portrayed as it would have looked shrunk onto the shaft without the presence of an expansion ring; the dotted line A' would be the seal's inner diameter with the shaft removed. When a ring is inserted at the outer end of the seal so as to stretch the ID of the seal, as shown in Figure 2-2(b), a flared opening is created at the end. Barring the presence of a lubricant, a reciprocating shaft would rub against the seal except over the ring-induced gap. Part (c) of Figure 2-2 portrays seal operation when a fluid film is present, and its hydrodynamic pressures separate shaft and seal during the forward stroke. The stresses and pressures corresponding to these three operational modes are shown in Figure 2-3.

2.2 The Elasticity Equation

Without the presence of a hydrodynamic film the configuration of the seal is determined approximately by the elasticity equation for an axisymmetric shell.

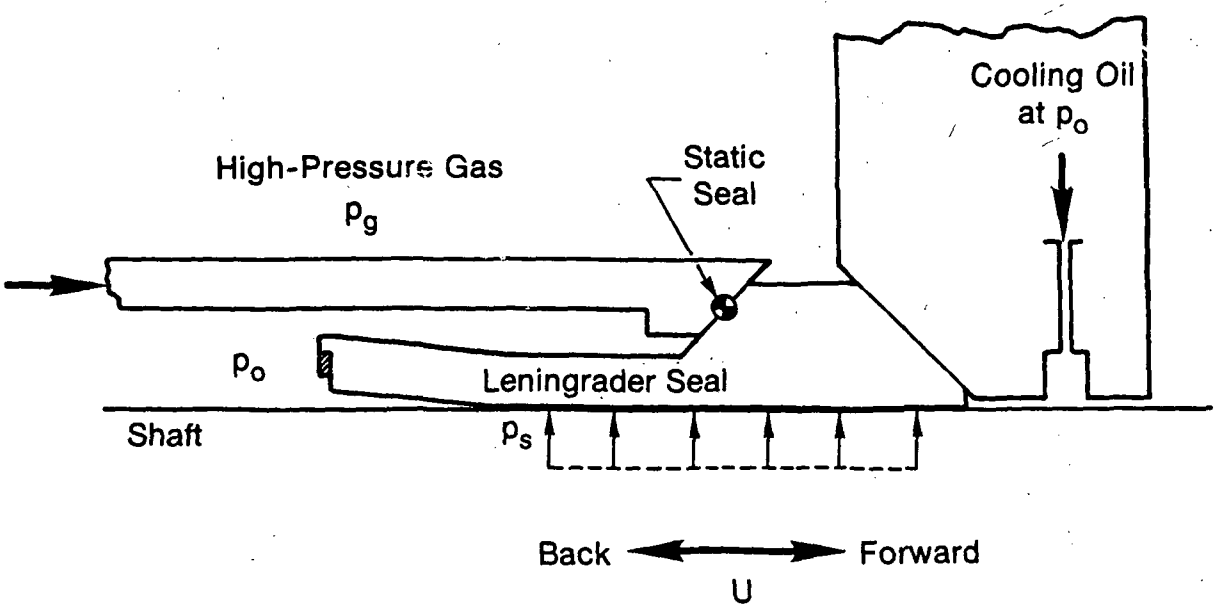
Cooling Oil
at p_o
High-Pressure Gas
p_g
Static
Seal
p_o
Leningrader Seal
Shaft
p_s
Back
Forward
U

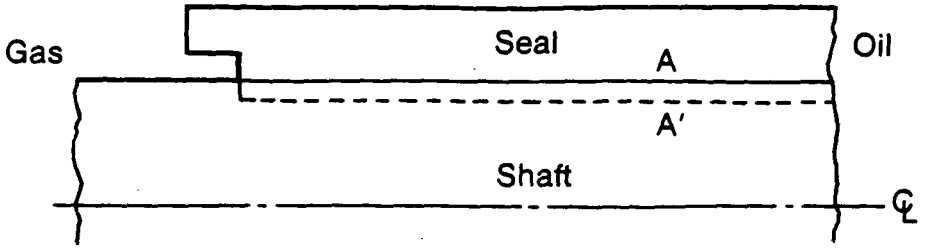

a) Interference — No Ring

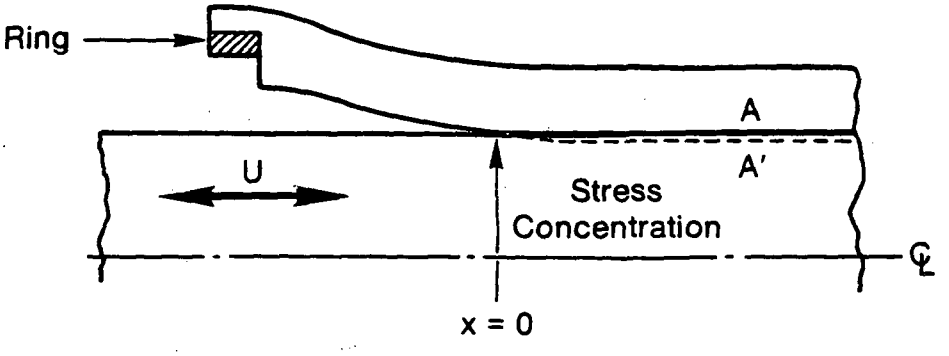

b) Ring Present — Rubbing Contact

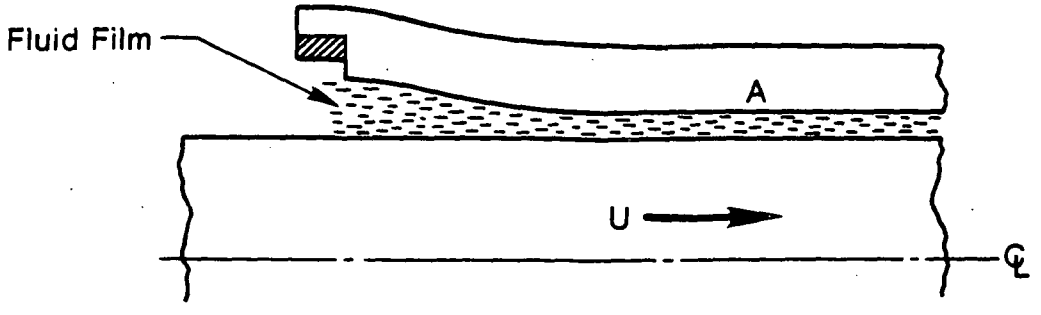

c) Ring Present — Hydrodynamic Film

Fig. 2-2 Mathematical Model of Leningrader Seal

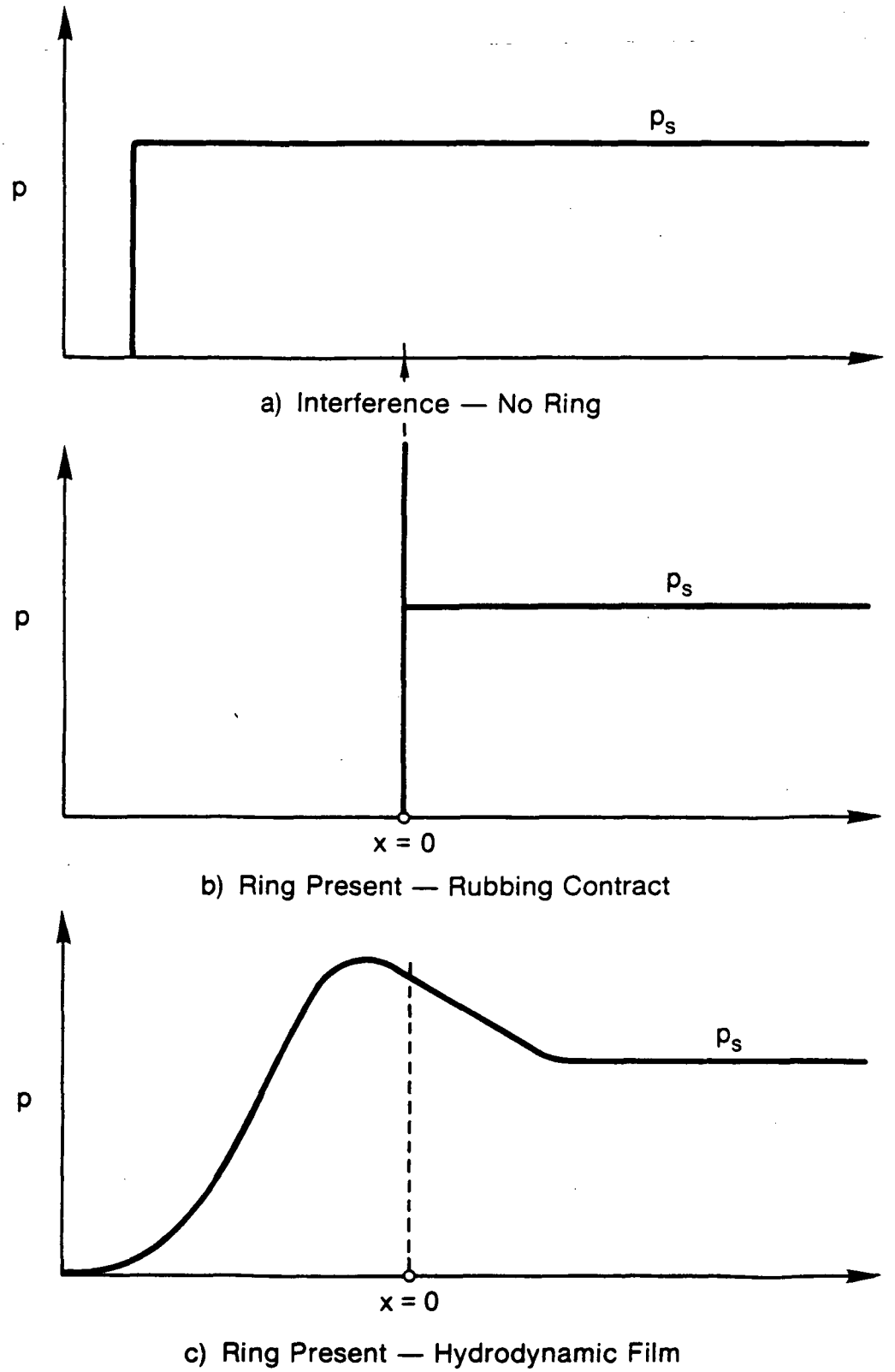

Fig. 2-3 Stresses or Pressures in Mathematical Model

$$D \frac{d^4 w}{dx^4} + \left(\frac{Et}{R^2}\right) w = p_g - p_o \tag{1}$$

where the flexural rigidity $D = Et^3/12(1-\nu^2)$. With the nomenclature specified in Figure 2-4, the boundary conditions are

$$x = 0; \qquad w = -\delta_s \qquad w' = w'' = 0$$

$$x = -L_r; \qquad w = -\delta_2 \qquad w' = 0$$

with the extra condition serving to determine L_r, an unknown. The solution to equation (1) will be in the form of $w = w(x)$, thus $\delta_r = \delta_r (L_r)$, and the expression would have to be inverted to obtain L_r in terms of the known input δ_r.

In dimensionless form the differential equation confined to the interval $0 < \bar{x} < \bar{L}_r$ becomes

$$\frac{d^4 \bar{w}}{d\bar{x}^4} + \bar{w} = 0 \qquad 0 < \bar{x} < \bar{L}_r \tag{2}$$

where $\bar{w} = -\left(\frac{w - \delta_o}{\delta_s + \delta_o}\right)$, with $\delta_o = \frac{R^2 (p_g - p_o)}{Et}$

The dimensionless coordinate $\bar{x} = -(x/\ell_e)$ has reversed the direction of the positive and negative x axes; and the normalizing factor ℓ_e is a diffusion length

$$\ell_e = \left(\frac{R^2 D}{Et}\right)^{1/4} = \frac{\sqrt{Rt}}{[12\ (1 - \nu^2)]^{1/4}}$$

representing the extent over which an applied force or stress makes itself felt in the seal's shell-like structure.

The boundary conditions in dimensionless form become

$$\bar{x} = 0;\ \bar{w} = 1,\ \bar{w}' = \bar{w}'' = 0 \tag{3a}$$

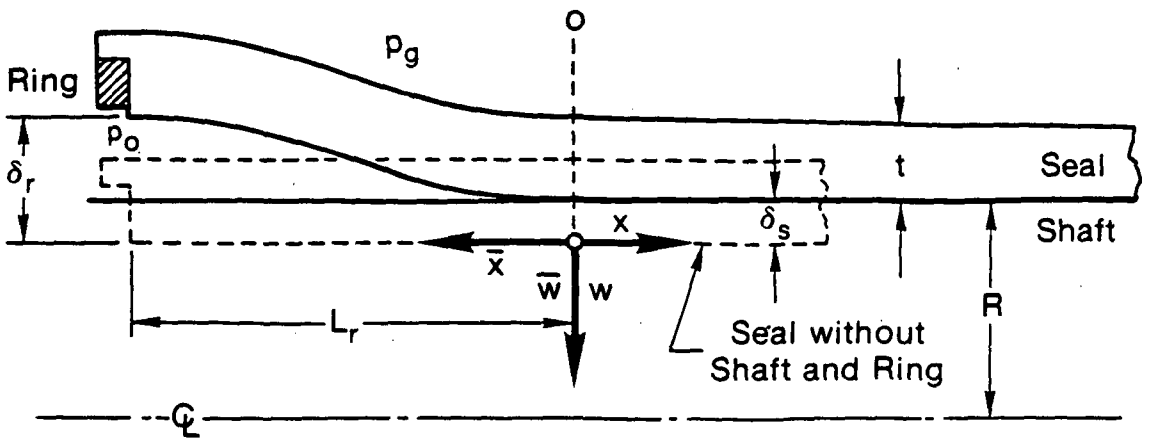

Fig. 2-4 Nomenclature for Seal Configurations

$$\bar{x} = (L_r/\ell_e);\ \bar{w} = (\delta_r + \delta_o)/(\delta_s + \delta_o),\ \bar{w}' = 0 \tag{3b}$$

The above is a fourth order linear differential equation and its solution is of the form

$$\bar{w} = \sum_{j=1}^{4} C_j\, e^{\lambda_j \bar{x}} \tag{4}$$

where

$$\lambda_j = \frac{1}{\sqrt{2}} \begin{Bmatrix} 1 + i \\ 1 - i \\ -1 + i \\ -1 - i \end{Bmatrix}$$

with the constant C_j determined by

$$\begin{bmatrix} 1 & 1 & 1 & 1 \\ \lambda_1 & \lambda_2 & \lambda_3 & \lambda_4 \\ \lambda_1^2 & \lambda_2^2 & \lambda_3^2 & \lambda_4^2 \\ \lambda_1 e^{\lambda_1 \bar{L}_r} & \lambda_2 e^{\lambda_2 \bar{L}_r} & \lambda_3 e^{\lambda_3 \bar{L}_r} & \lambda_4 e^{\lambda_4 \bar{L}_r} \end{bmatrix} \begin{Bmatrix} C_1 \\ C_2 \\ C_3 \\ C_4 \end{Bmatrix} = \begin{Bmatrix} 1 \\ 0 \\ 0 \\ 0 \end{Bmatrix}$$

Substituting in (4) $w = \delta_r$ we obtain

$$\left(\frac{\delta_r + \delta_o}{\delta_s + \delta_o}\right) = \sum_{j=1}^{4} C_j e^{\lambda_j (L_r/\ell_e)} \tag{5}$$

which is the desired expression for L_r in terms of δ_r.

Figures 2-5 and 2-6 show the extent of lift-off L_r in terms of both the ratio of the interferences (δ_r/δ_s) and their difference $(\delta_r - \delta_s)$. It is seen that most of the length of L_r is formed at the very beginning. When $\delta_r = 2\delta_s$, $\bar{L}_r = 2.75$; when $\delta_r = 10\delta_s$, $\bar{L}_r = 3.9$. Thus a fivefold increase in δ_r produces only a 42% rise in extent of L_r. The shear on the other hand, except at the very

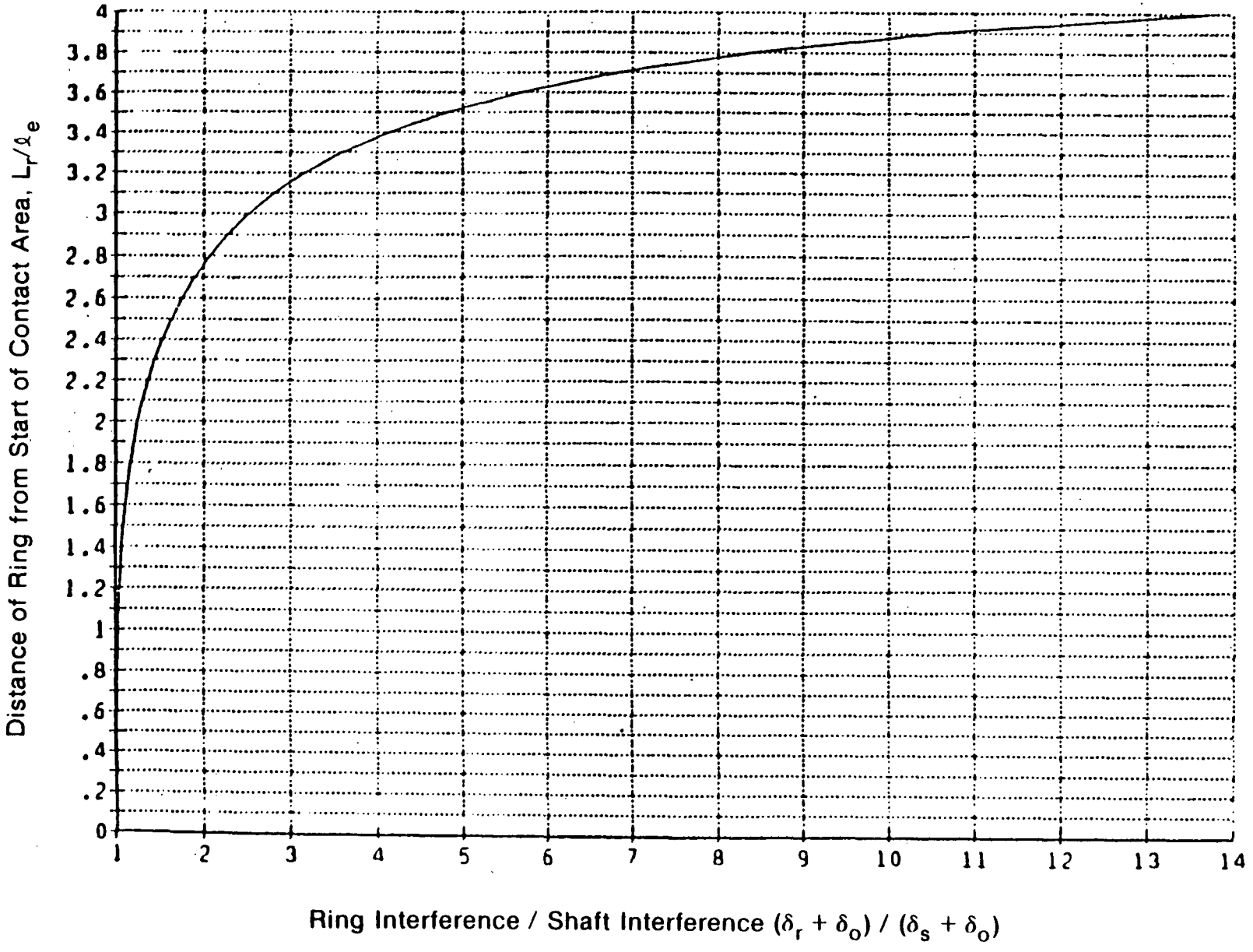

Fig. 2-5 Relation Between Extent of Lift-off and Interferences

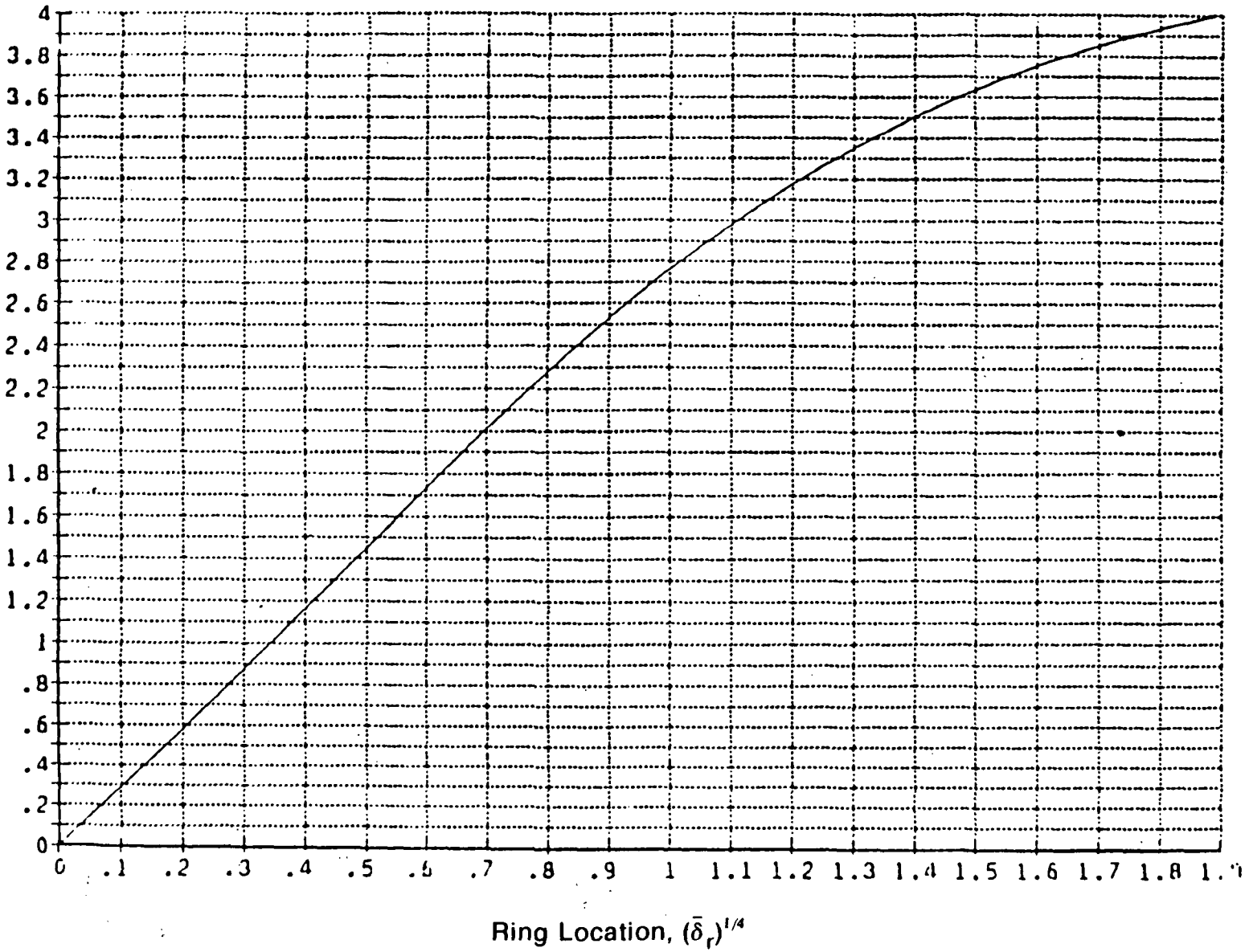

Fig. 2-6 Extent of Lift-off as Function of Size of Ring

beginning, rises about linearly with an increase in δ_r, as shown in Figures 2-7 and 2-8. At the beginning it behaves similarly to the lift-off, that is a small increase in δ_r produces a rapid rise in the shearing force at the point of contact x = 0.

2.3 Elastohydrodynamic Solution

2.3.1 The Governing Equations

When there is a hydrodynamic fluid film h, its thickness, sketched in Figure 2-9, is related to w via

$$w = -(h + \delta_s) \tag{6}$$

where δ_s is a constant. The previously constant pressure p_o in the gap is now replaced by the hydrodynamic pressure p(x). When these are introduced into equation (1), we obtain the elasticity equation in terms of h and p(x), namely

$$D\frac{d^4h}{dx^4} + \frac{Et}{R^2}h = p(x) - p_g - \left(\frac{Et\delta_s}{R^2}\right) \tag{7}$$

The hydrodynamic pressures p(x) are obtainable from the one-dimensional Reynolds equation which, when integrated once, yields

$$\frac{dp}{dx} = 6\mu U\left(\frac{h - h_o}{h^3}\right) \tag{8}$$

with h_o a constant of integration to be determined.

The boundary conditions for this EHD problem are

$$x = -L_r;\ p = p_g,\ h = (\delta_s + \delta_r),\ h' = 0 \tag{9a}$$

$$x \to \infty\ ;\ p = p_g + \frac{Et}{R^2}(h_s + h_o)^*,\ h = h_o \tag{9b}$$

*This term represents the hoop stresses in the seal which must be balanced by the hydrodynamic pressures.

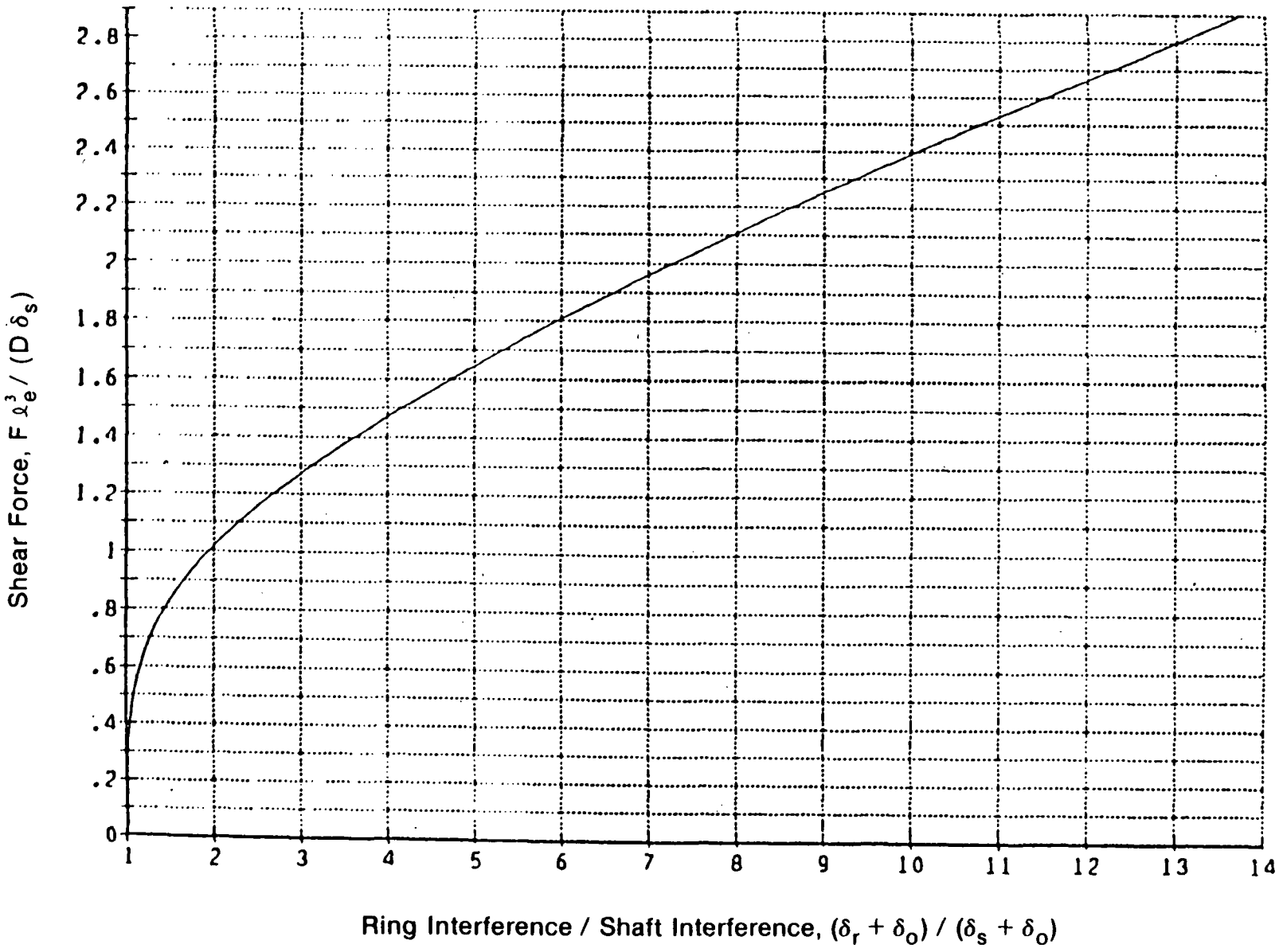

Fig. 2-7 Shear Force at Contact Point as Function of Interferences

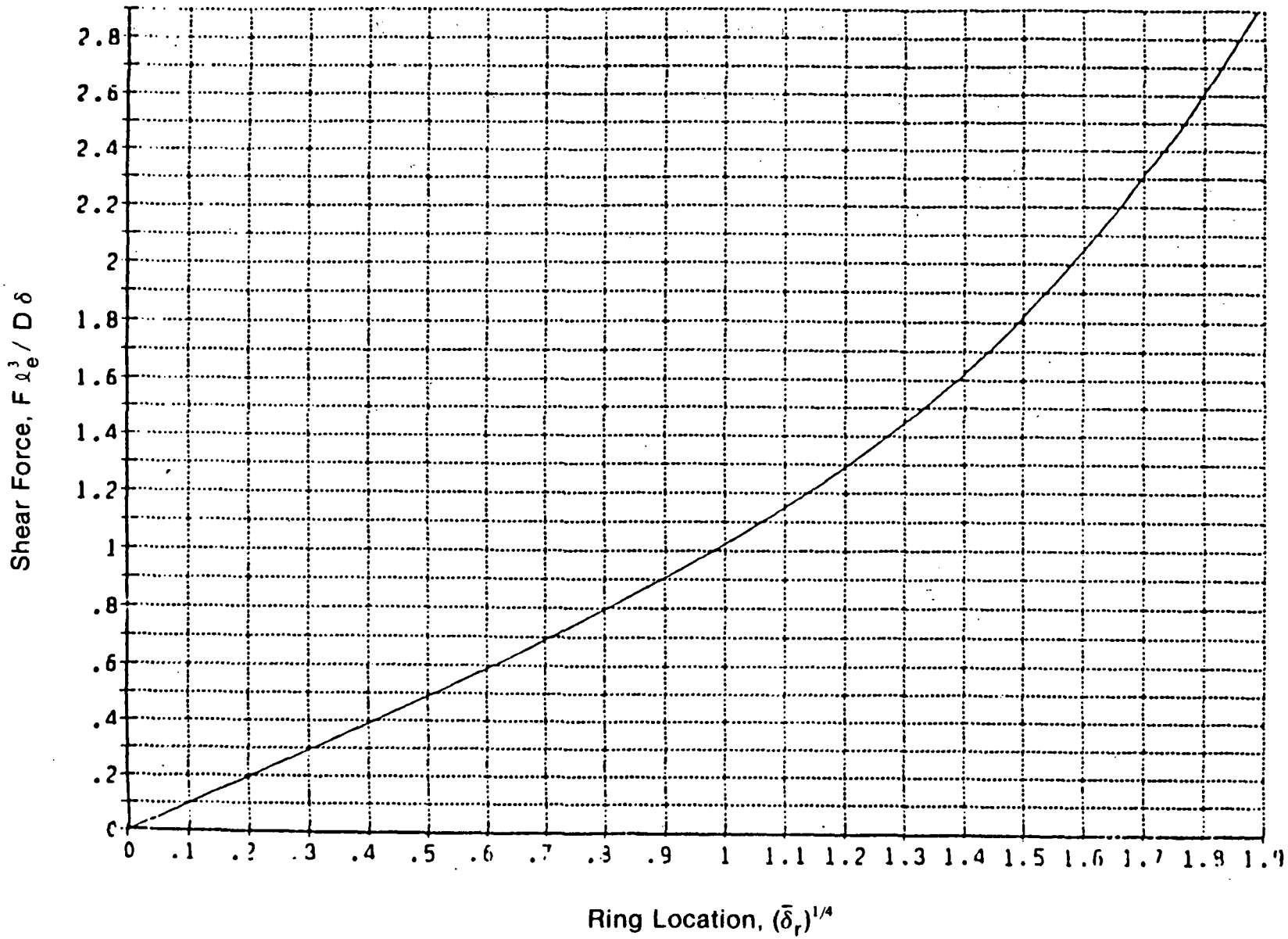

Fig. 2-8 Shear Force at Contact Point as Function of Size of Ring

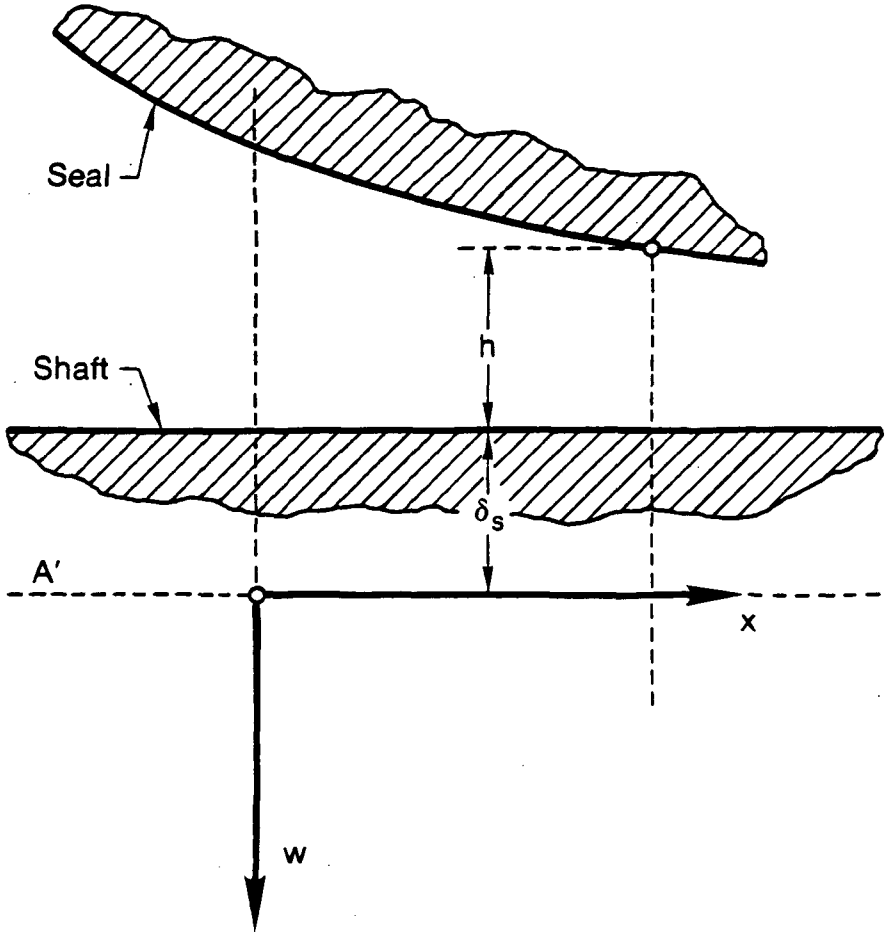

Fig. 2-9 Hydrodynamic Fluid Film Thickness

In normalized form, the two differential equations and their boundary conditions become

$$\frac{d^4\hat{h}}{d\bar{x}^4} + \hat{h} = \hat{p} \tag{10}$$

$$\frac{d\hat{p}}{d\bar{x}} = -\beta \frac{\hat{h}}{(1+\hat{h})^3} \tag{11}$$

$$\bar{x} = \bar{L}_r;\ -\hat{p} = 1 + \left(\frac{\delta_s + \delta_o}{h_o}\right),\ \hat{h} = (\delta_r - \delta_s - h_o)/h_o \quad \frac{d\hat{h}}{d\bar{x}} = 0 \tag{12a}$$

$$\bar{x} \to \infty;\ \lim \hat{p} = 0,\ \lim \hat{h} = 0 \tag{12b}$$

where

$$\beta = \frac{6\mu\, U\, \ell_e\, \delta_s}{h_o^3\, p_s} = \frac{6\mu\, U\, \ell_e\, R^2}{h_o^3\, E t_o^3}$$

will be referred to as the EHD parameter.

Boundary conditions (12a) yield also the following useful relationships

$$\left(\frac{\delta_s + \delta_o}{h_o}\right) = -(1 + \hat{p}) \tag{13a}$$

$$\bar{\delta}_r = -\left(\frac{1+\hat{h}}{1+\hat{p}}\right) \tag{13b}$$

$$\beta_1 = \frac{\beta}{(1+\hat{p})^3} \tag{13c}$$

Other relationships between the normalized quantities are

$$\bar{p} = -\frac{\hat{p} - \hat{p}\ (\bar{L}_r)}{1 + \hat{p}\ (\bar{L}_r)} \tag{13d}$$

$$\bar{h} = -\frac{1 + \hat{h}}{1 + \hat{p}\ (\bar{L}_r)} \tag{13e}$$

$$\bar{p}\left(\frac{\delta_s + \delta_o}{h_o}\right) = \hat{p} - \hat{p}\ (\bar{L}_r) = \hat{p} + 1 + \left(\frac{\delta_s + \delta_o}{h_o}\right) \equiv \tilde{p} \tag{13f}$$

2.3.2 Solution of EHD Problem

The origin of the coordinate system is here moved far upstream where $h \simeq h_o$, as shown in Figure 2-10. Under these conditions $\hat{h} << 1$ and so in the denominator of equation (11), $\hat{h}$ can be ignored relative to 1. Differentiating equation (10) and substituting for $(d\hat{p}/d\bar{x})$ from equation (11) we obtain

$$\frac{d^5\hat{h}}{d\bar{x}^5} + \frac{d\hat{h}}{d\bar{x}} + \beta\hat{h} = 0 \tag{14}$$

a linear equation in $\hat{h}\ (\bar{x})$. The solution to this differential equation is of the form

$$\hat{h}\ (\bar{x}) = \sum_{j=1}^{5} A_j e^{m_j \bar{x}}$$

where m_j are the roots of the 5th order polynominal

$$m^5 + m + \beta = 0 \tag{15}$$

Since $\hat{h}\ (\bar{x}) \to 0$ as $\bar{x} \to -\infty$ we are allowed to retain only those roots that have positive real parts. It can be shown that equation (15) has only two such roots, a conjugate pair of complex numbers λ and $\bar{\lambda}$. Combining these two roots the solution then becomes

$$\hat{h} = \epsilon\ \mathrm{Re}\ [e^{\lambda\bar{x} + i\phi}] \tag{16}$$

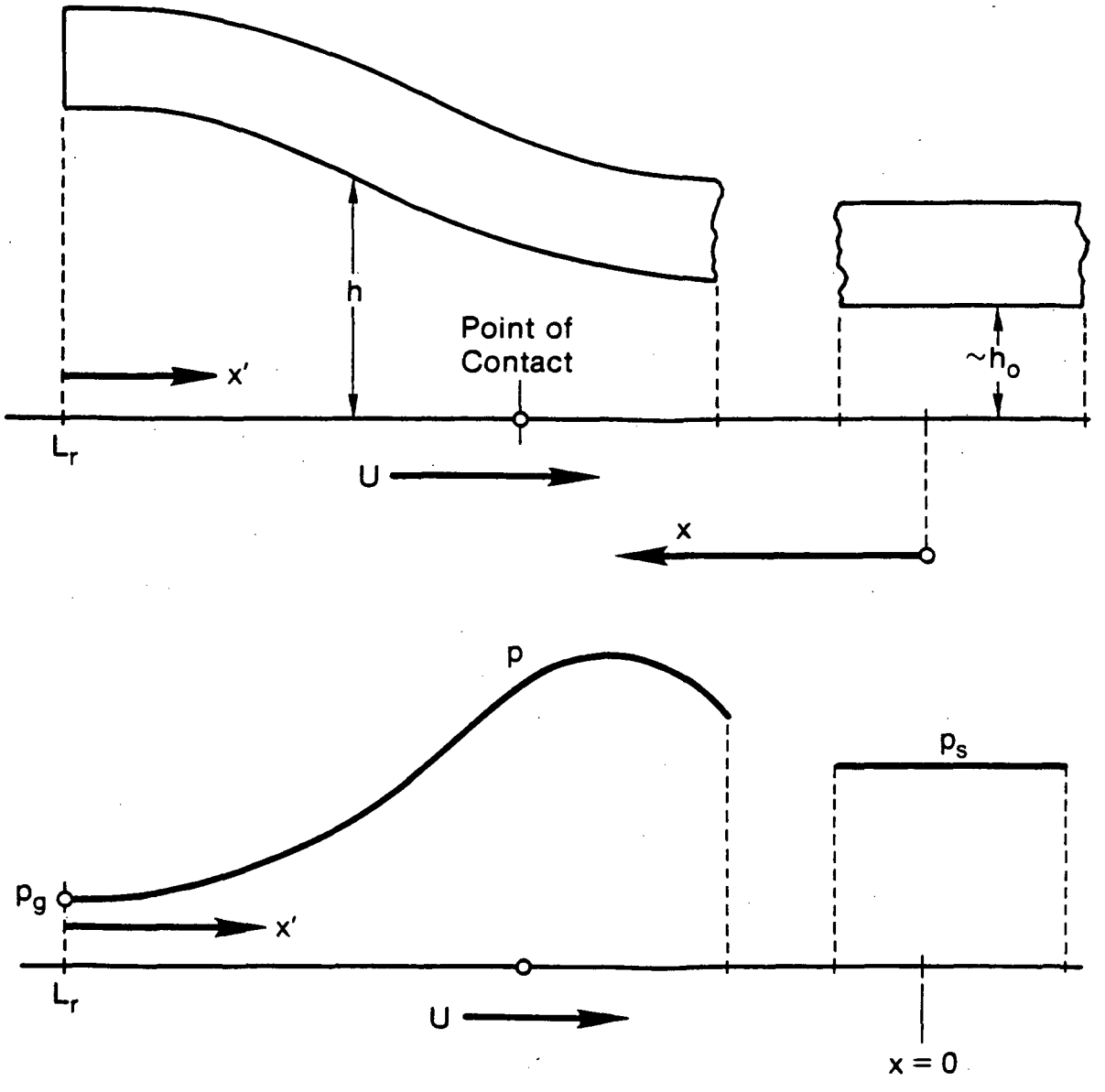

Fig. 2-10 The EHD Fluid Film

where ϵ and ϕ are real and λ is one of the two roots of equation (15), namely the one having positive constants in both the real and imaginary parts. Thus

$$h(0) = \epsilon \cos \phi$$

$$\hat{h}^{(n)}(0) = \epsilon \, \mathrm{Re} \, (\lambda^n \, e^{i\phi}) \qquad \text{(n-th derivative)}$$

In order to proceed with obtaining a solution, certain initial values are needed. We employ the following:

- ϵ is assigned some small value, say 0.01
- For any given β, λ is determined from equation (15)
- For any given value of ϕ, values of $\hat{h}$ and its derivatives $\hat{h}^{(n)}$ are determined for use as boundary conditions at $\bar{x} = 0$ in equations (10) and (11).

The above are used as starting points for a Runge-Kutta solution to equations (10) and (11). The stepwise method is continued until $(d\hat{h}/d\bar{x})$ changes sign. We then

- Obtain the corresponding value at L_r by quadratic interpolation.
- Carry out the Runge-Kutta integration over the range $0 - \bar{L}_r$.
- Obtain values of $\bar{\delta}_r$ and β from equations (13b) and (13c), respectively, which in this form are functions of ϕ and β and thus must be inverted. However, it seems more efficacious to simply obtain direct computations of $\bar{\delta}_r$ and β_1 as functions of ϕ and β.

2.3.3 Parametric Solutions

The system under study here is well covered by the following ranges:

$$0.5 < \delta_r < 50$$

$$10^2 < \beta < 10^5$$

The relations between these parameters and the variables ϕ and β_1 are given in Figures 2-11 and 2-12. As seen, for large β, the $\bar{\delta}_r$ = constant lines are nearly parallel and we may thus approximate β by

$$\beta_a = \left(\frac{C}{\beta_1}\right)^{1.2203}$$

where C is plotted in Figure 2-13. The deviation of β from β_a is shown in Figure 2-14.

Single variable interpolation of the results shown in Figure 2-4 and bivariate interpolation of Figure 2-14 are used to compute β. ϕ is then computed from β by a bivariate interpolation of the results in Figure 2-12.

Figures 2-15 and 2-16 give the major items of interest in the EHD problem, namely the shapes and extents of the fluid film and its hydrodynamic pressures, for the case of $\beta_1 = 0.2$. As seen, the parallel film portion is reached at a distance of 3 to 4 times ℓ_e. The pressures all peak about the point where $(dh/dx) \to 0$ and are therefore located very near the point where contact would have occurred in the absence of a fluid film. As seen from Figure 2-17 the location of p_{max} is very little affected by β and only mildly by $\bar{\delta}_r$; a five-fold increase in δ_r produced a shift in x_m of 20% for the 2 to 10 shift, and only 10% for the 10 to 50 shift in $\bar{\delta}_r$.

2.4 Solution with Seal Wear Included

2.4.1 The Elasticity Equation

It was postulated earlier, in Figure 2-2, that at the point of contact an infinite shear prevails. In practice this is unlikely as under such heavy loading the motion of the shaft would produce a high rate of wear at the initial point of contact and the shear concentration would be relieved.

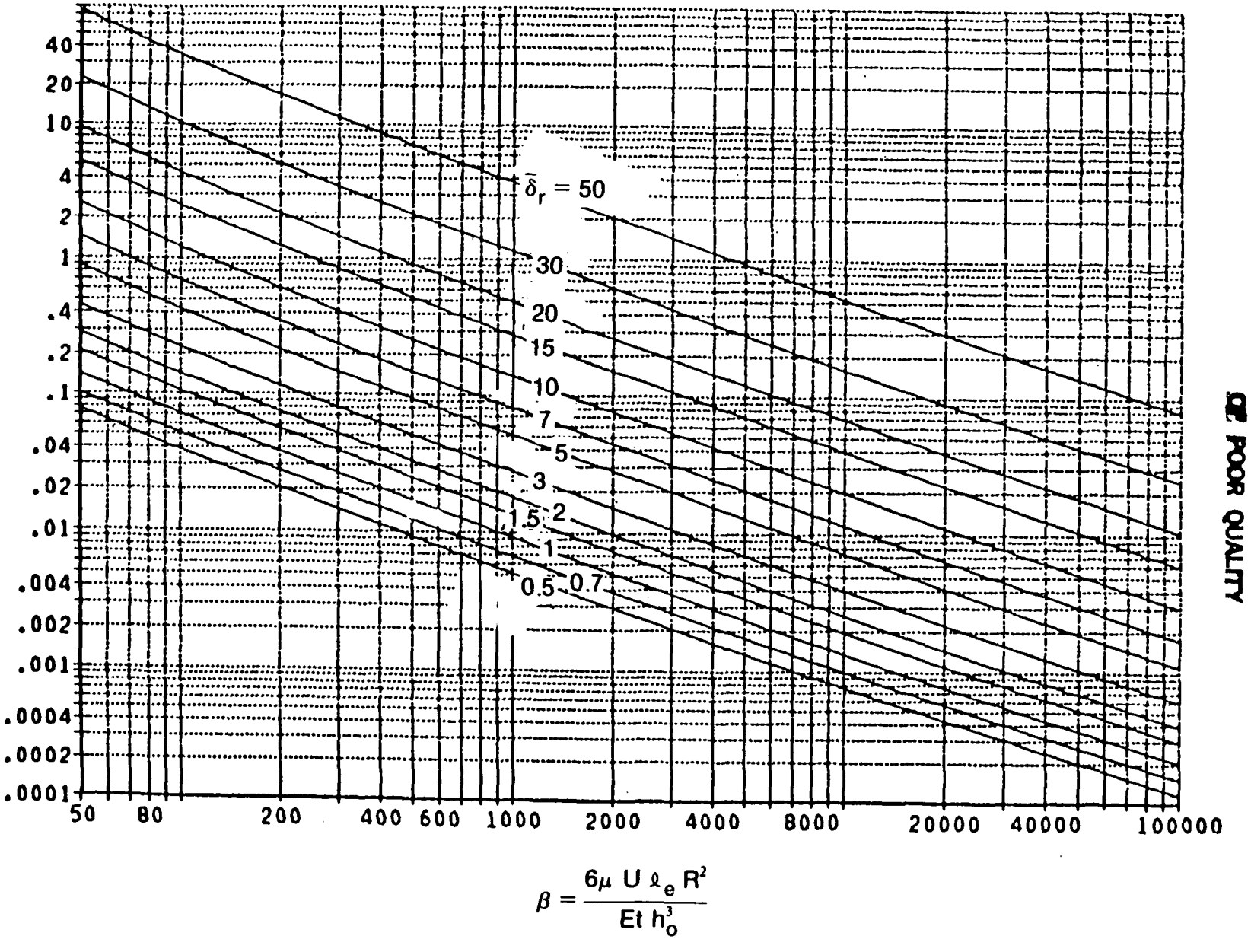

Fig. 2-11 Relation Between β_1 and Parameters $\bar{\delta}_r$ and β

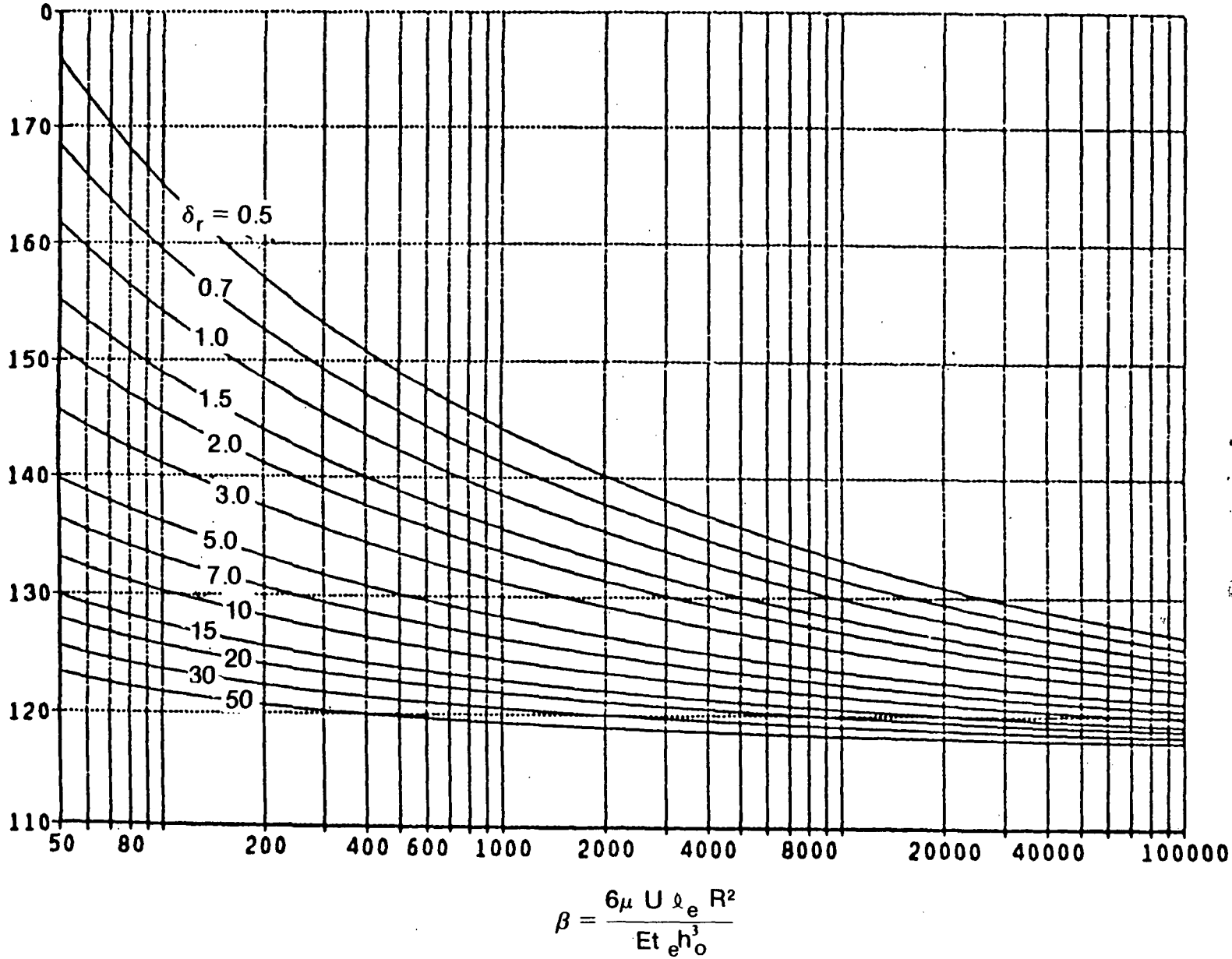

Fig. 2-12 Relation Between ϕ and Parameters $\bar{\delta}_r$ and β

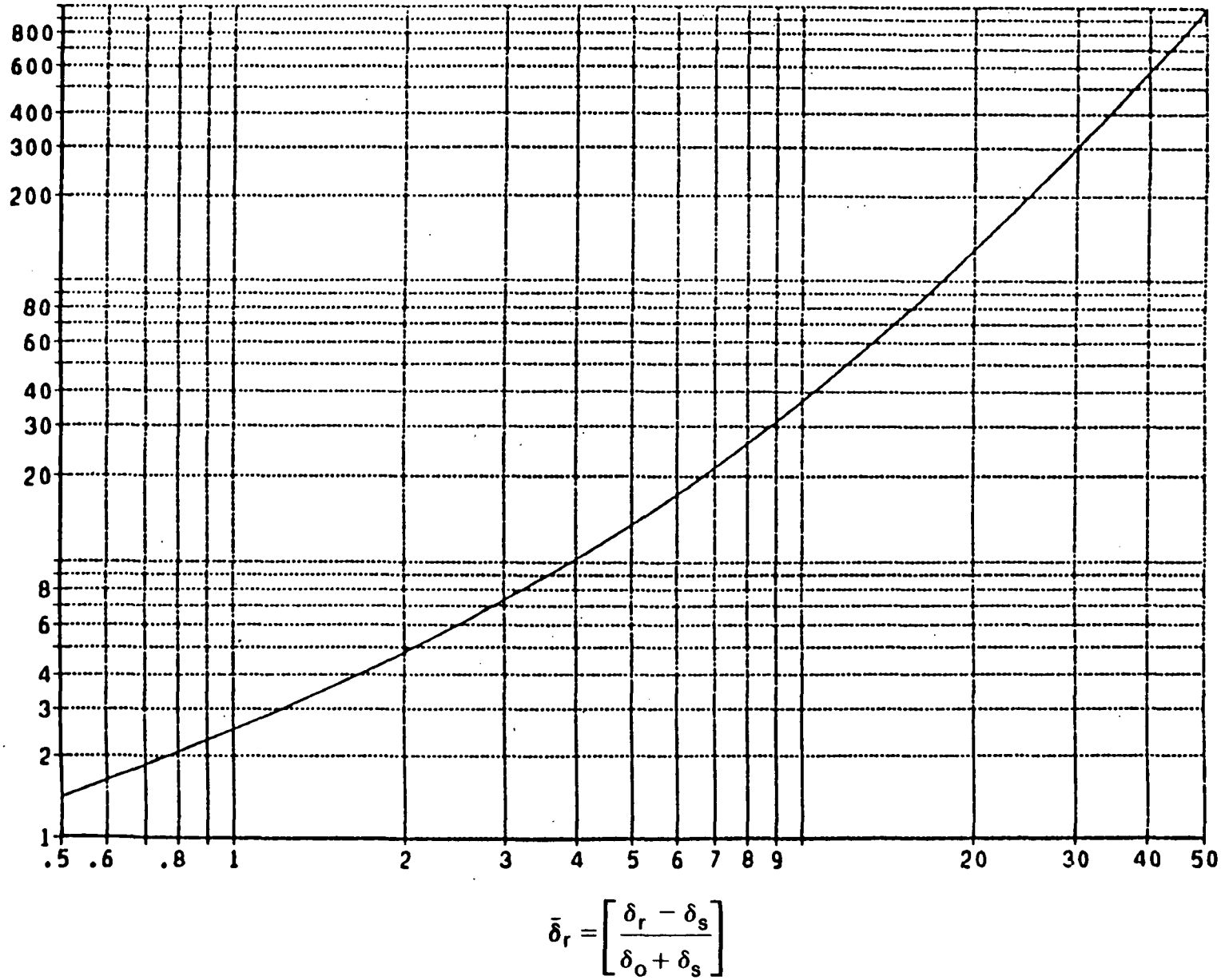

Fig. 2-13 Value of Constant C in $\beta_a = (C/\beta_1)^{1.2203}$

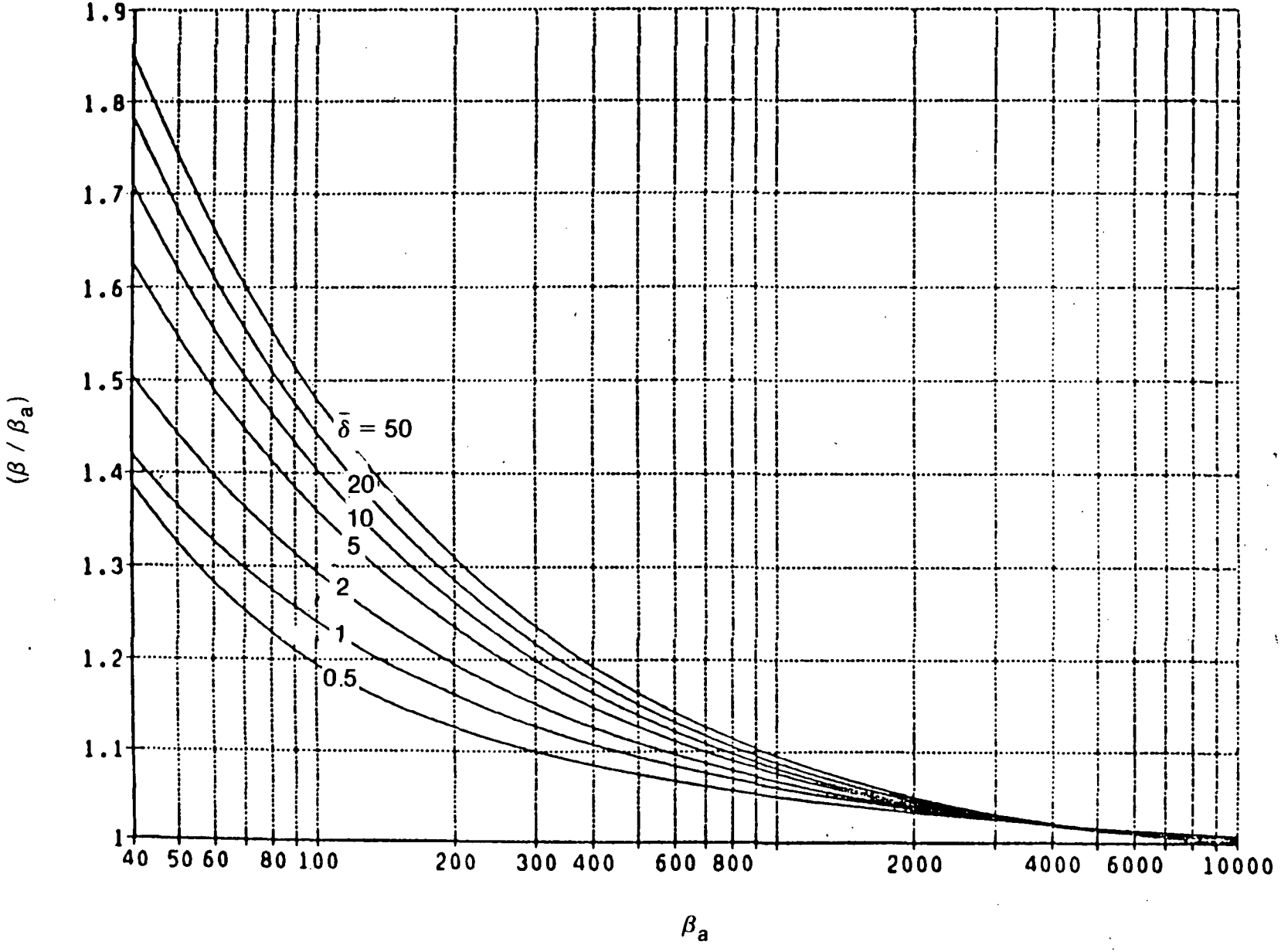

Fig. 2-14 Approximate and Exact Values of β

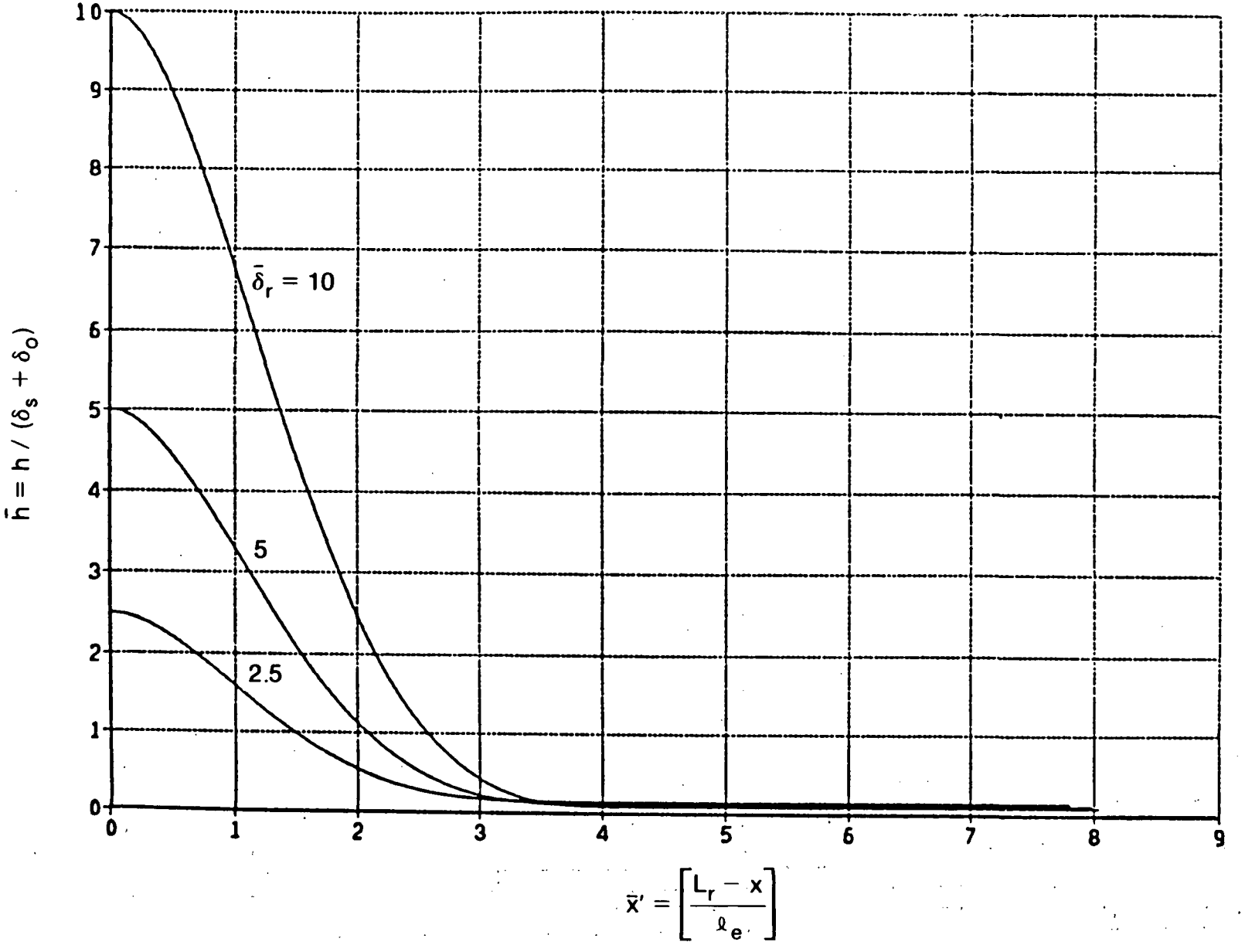

Fig. 2-15 Inlet Film Thickness Profile at $\beta_1 = 0.2$

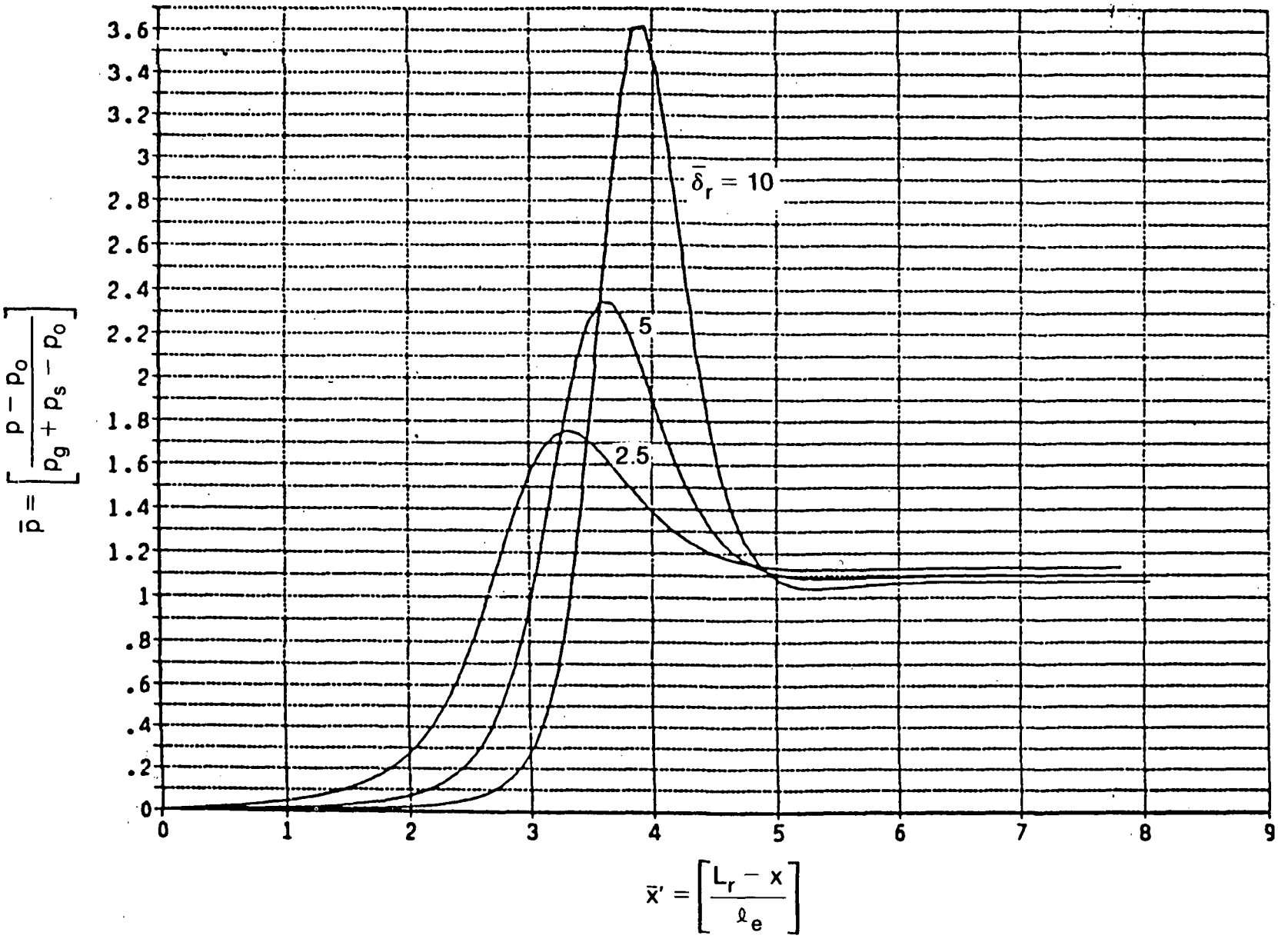

Fig. 2-16 Pressure Profiles for $\beta = 0.2$

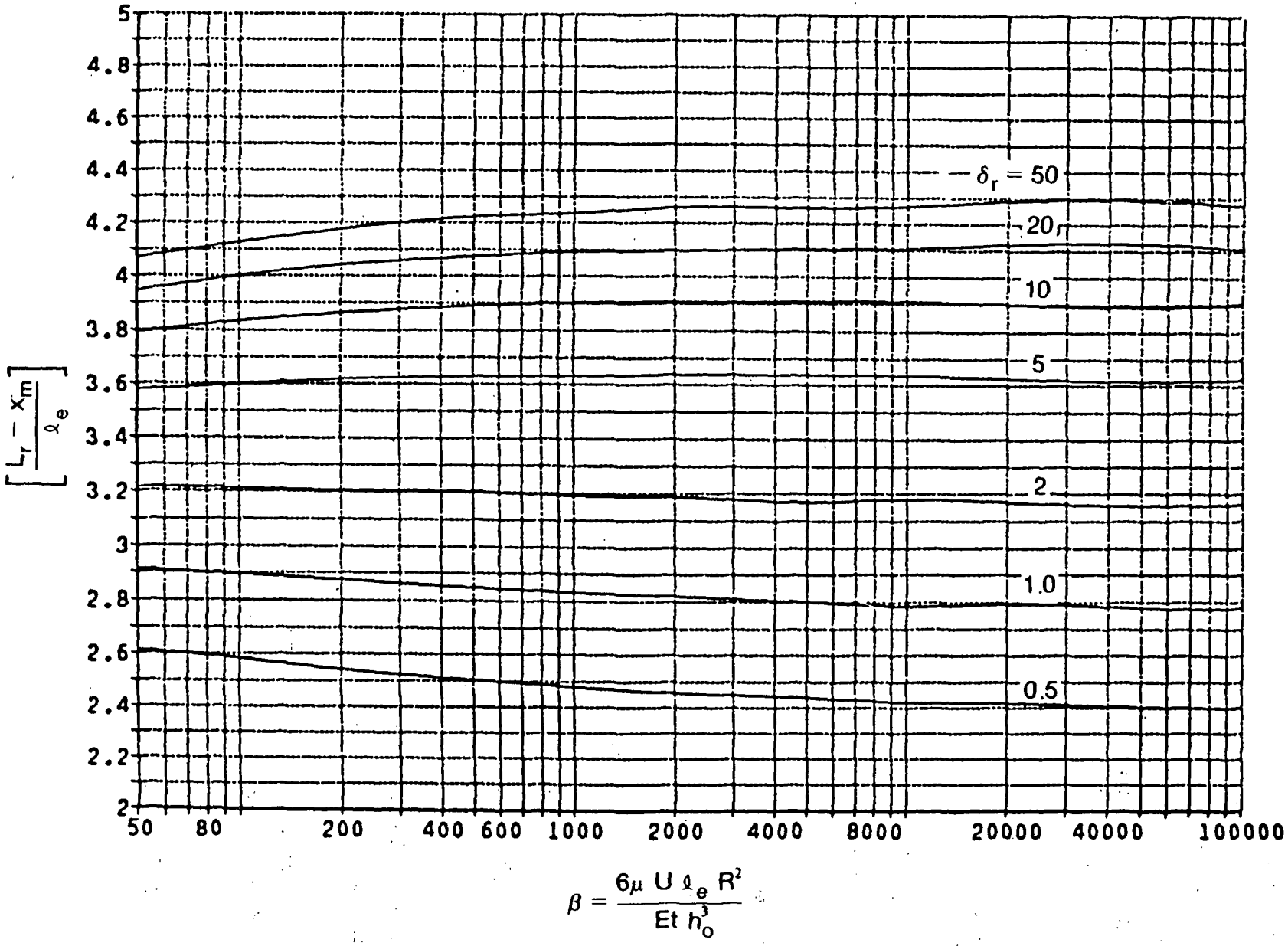

Fig. 2-17 Location of Maximum Pressure as Function of $\bar{\delta}_2$ and β

This situation is portrayed graphically in Figure 2-18 where the shaded areas represent the amount of material removed by wear. Without wear, as postulated in previous sections, that amount of shaded seal substance would have had to be displaced above the shaft surface, thus causing the high shear concentration at the initial point of contact. Now, with that amount of interferring matter removed, the stress is relieved so that, over the entire contact area, a uniform stress p_s prevails.

The differential equation now reads for the two separate regions bounded by $x = 0$

$$D\frac{d^4w}{dx^4} + \frac{Et}{R^2}w = \begin{cases} (p_g - p_o), & -L_r < x < 0 \quad (17a) \\ -p_s, & 0 < x < \infty \quad (17b) \end{cases}$$

The boundary conditions are:

$$x = -L_r; \quad w = -\delta_r, \; w' = 0 \quad (18a)$$

$$x = 0; \quad w, \; w', \; w'', \text{ and } w''' \text{ are continuous} \quad (18b)$$

$$x = \infty \quad \begin{cases} \lim w = -\delta_s \\ \lim w', \; w'', \; w''' = 0 \end{cases} \quad (18c)$$

Essentially the new condition introduced here is that the shear (w''') goes to zero at $x = 0$ along with the lower derivatives.

In dimensionless form and with the reversed direction of the x axis the differential equation and the boundary conditions become

$$\frac{d^4w}{d\bar{x}^4} + \bar{w} = \begin{cases} 0, & \bar{x} > 0 \quad (19a) \\ 1, & \bar{x} < 0 \quad (19b) \end{cases}$$

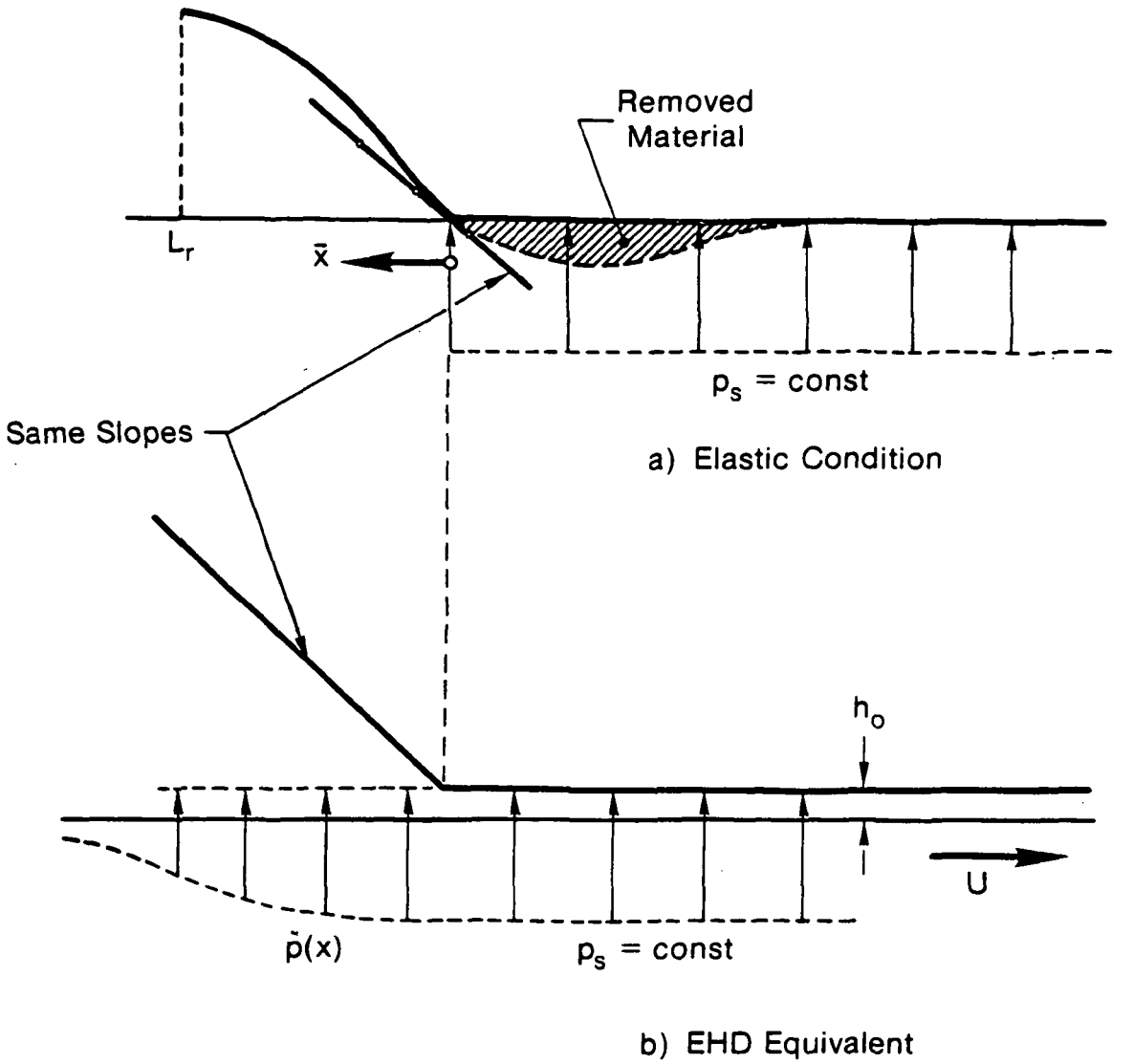

Fig. 2-18 The EHD Problem with Wear Included

$$\bar{x} = \bar{L}_r;\ \bar{w}' = 0 \tag{20a}$$

$$\bar{x} \to -\infty \quad \lim w = \delta, \quad \lim \bar{w}', \bar{w}'', \bar{w}''' = 0 \tag{20b}$$

with all the derivatives continuous at $\bar{x} = 0$.

The solutions to equations (19a) and (19b) are

$$\bar{w} = \sum_{j=1}^{4} C_j' e^{\lambda_j \bar{x}} \qquad \bar{L}_r > x > 0 \tag{21a}$$

$$\bar{w} = 1 - \alpha\, e^{\frac{\bar{x}}{\sqrt{2}}} \sin\left(\frac{\bar{x}}{\sqrt{2}}\right) \qquad 0 > \bar{x} > -\infty \tag{21b}$$

where α is an unknown constant. The four coefficients C_j' and α can be obtained from use of the boundary conditions (20a) and (20b) yielding

$$\begin{bmatrix} 1 & 1 & 1 & 1 & 0 \\ \lambda_1 & \lambda_2 & \lambda_3 & \lambda_4 & 1/\sqrt{2} \\ \lambda_1^2 & \lambda_2^2 & \lambda_3^2 & \lambda_4^2 & 1 \\ \lambda_1^3 & \lambda_2^3 & \lambda_3^3 & \lambda_4^3 & 1/\sqrt{2} \\ \lambda_1 e^{\lambda_1 \bar{L}_r} & \lambda_2 e^{\lambda_2 \bar{L}_r} & \lambda_3 e^{\lambda_3 \bar{L}_r} & \lambda_4 e^{\lambda_4 \bar{L}_r} & 0 \end{bmatrix} \begin{Bmatrix} C_1' \\ C_2' \\ C_3' \\ C_4' \\ \alpha \end{Bmatrix} = \begin{Bmatrix} 1 \\ 0 \\ 0 \\ 0 \\ 0 \end{Bmatrix}$$

In the above, the zeros on the right-hand side of the matrix indicate not zero slopes but zero differences in slope at $\bar{x} = 0$, in accordance with the requirement of continuity of w', w'', and w''' at $x = 0$.

After obtaining the values of C_j' and α, the relation between $\bar{L}_r$ and $\bar{\delta}_r$ is obtained by first locating the value of $\bar{x}$ where $\bar{w}' = 0$, finding the corresponding value of w which then supplies $\bar{\delta}_r$ via

$$\bar{w} = \frac{\delta_r + \delta_o}{\delta_s + \delta_o} = 1 + \bar{\delta}_r \tag{22}$$

The shape of the separation gap due to seal wear in the vicinity of $\bar{x} = 0$ is portrayed in Figure 2-19. As seen, the extent of the lift-off gap had shrunk; and at the new point of contact the slope is no longer zero. The decrease in the separation length L_r and the increase in slope at contact point with a rise in $\bar{\delta}_r$ are given in Figures 2-20 and 2-21.

2.4.2 The Hydrodynamic Solution

The hydrodynamic solutions will here be approximated by representing the gap between the seal and shaft as equivalent to a composite axisymmetric bearing, as shown in Figure 2-18(b). The wedge-shaped portion of the bearing is given a slope equal to the slope of the seal at the initial point of contact with the shaft. The wedge can be made to extend to infinity, as with increasing h, the contribution to the pressures will decay rapidly. In the parallel portion of the bearing, the pressures must be constant and equal to p_s, the hoop stresses in the seal.

The details of solving this simple one-dimensional Reynolds equation with the proper boundary conditions are given in Reference 1. The solution for h_o, which is the main quantity desired, is also given in Reference 1 as Equation A-15, namely

$$h_o = \frac{3\mu U}{(p_s + p_g - p_o)\,\theta}$$

Writing for the bearing slope

$$\theta = \left(\frac{\delta_s + \delta_o}{\ell_e}\right) \bar{w}\,(0)$$

we obtain for the value of the hydrodynamic gap

$$h_o \simeq \frac{3\mu U\, \ell_e}{(\delta_o + \delta_s)\,\bar{w}'(0)\,(p_s + p_g - p_o)} \tag{23}$$

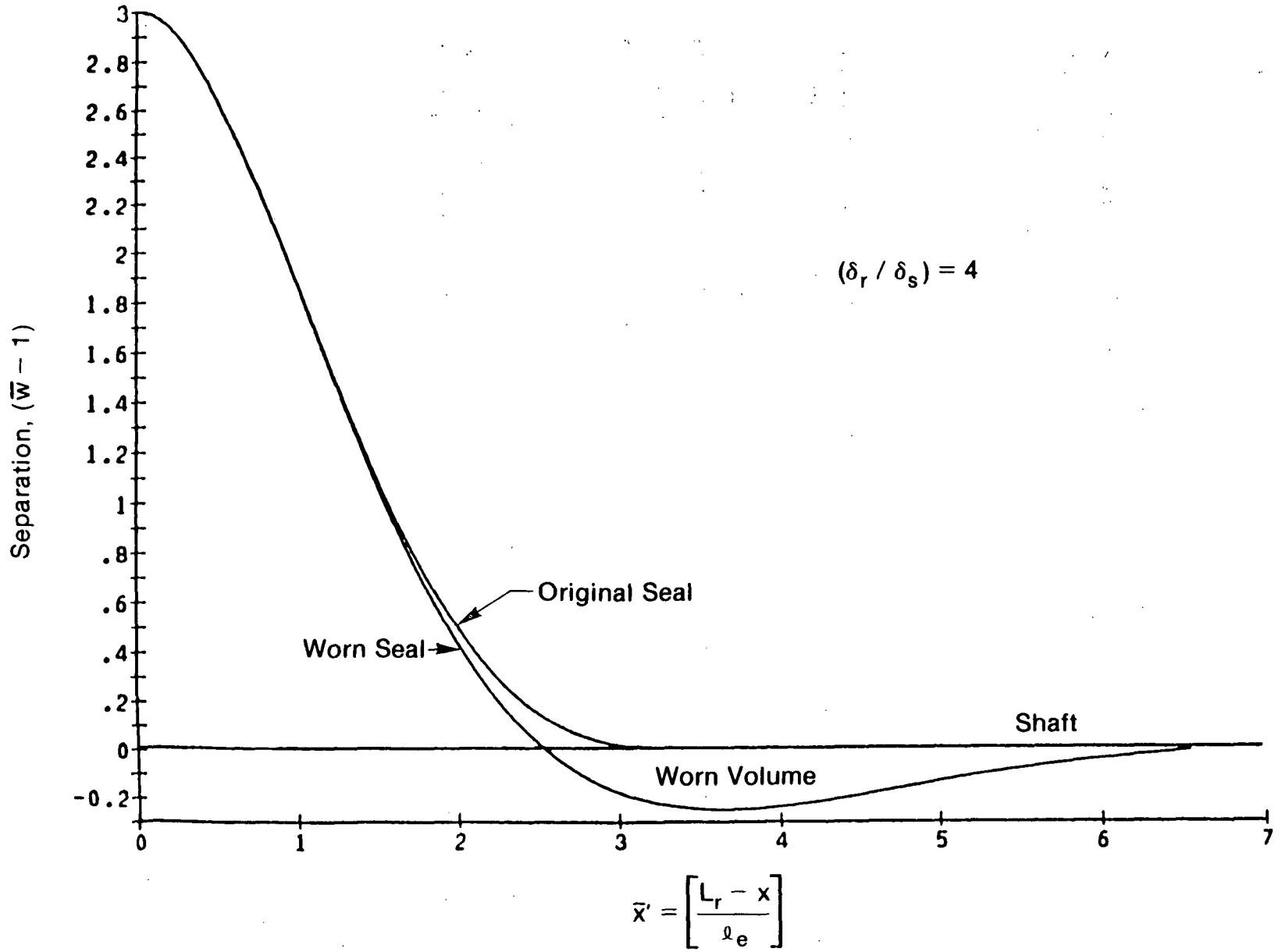

Fig. 2-19 Gap Geometrics for Worn and Unworn Seals

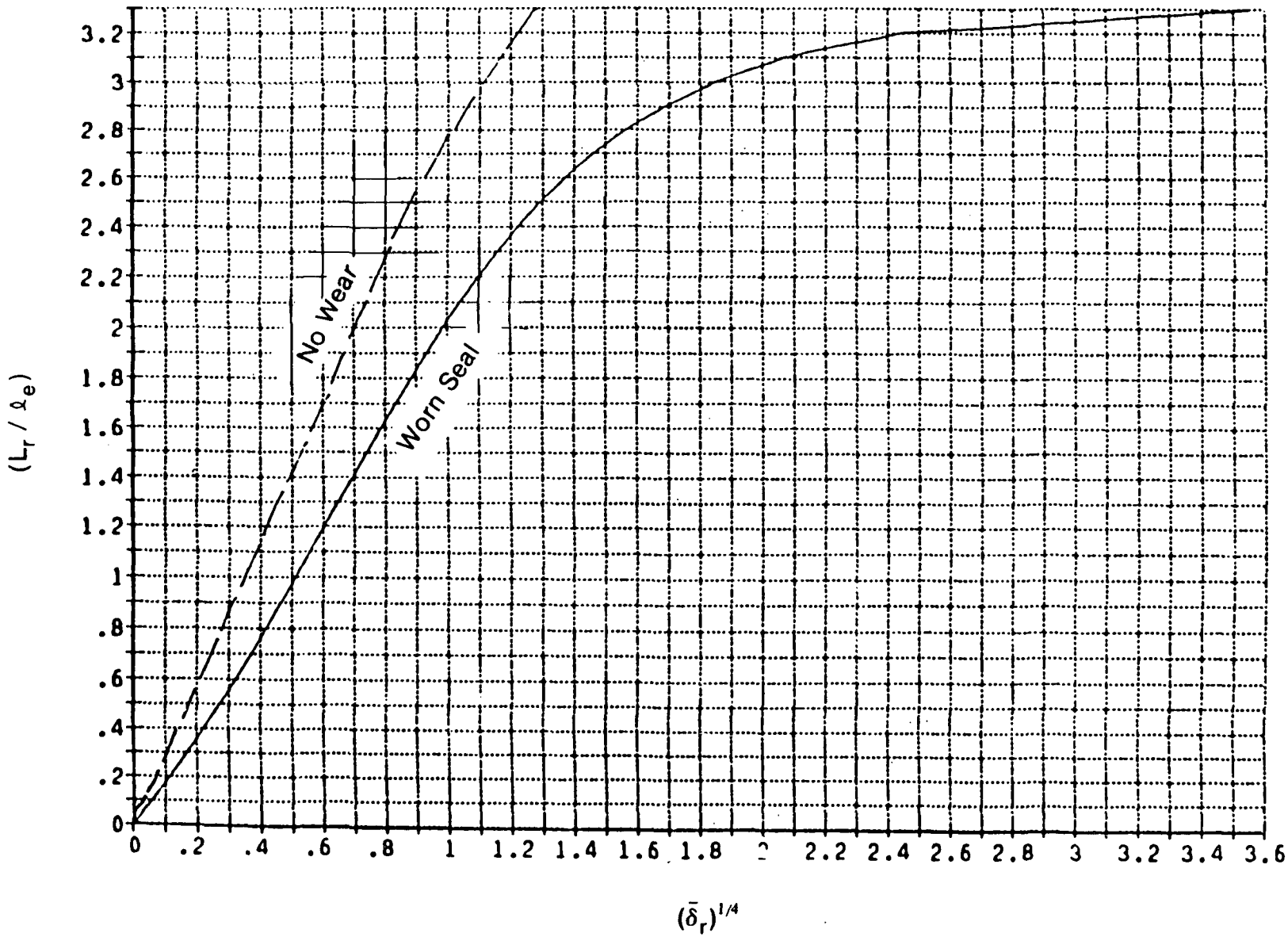

Fig. 2-20 Extent of Lift-off for Worn and Unworn Seals

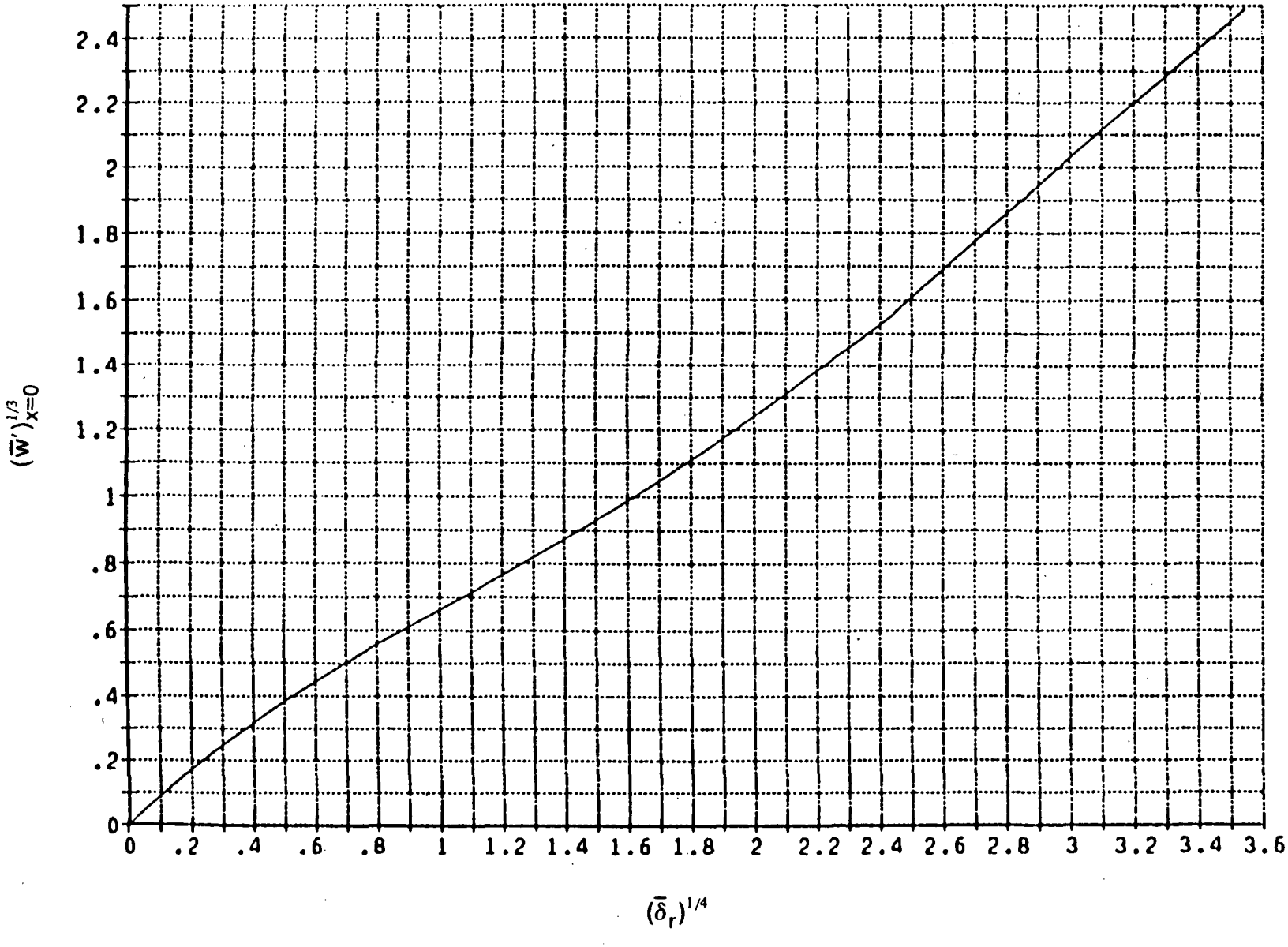

Fig. 2-21 Slope at x = 0 for Worn Seal

2.5 Numerical Computation

Computations of displacements and pressures occurring in a Leningrader seal are performed for a set of typical conditions as given in Table 2-1.

Figures 2-22 and 2-23 give the shapes and extents of the film thicknesses and pressure profiles for three levels of ring interference. The characteristics of the seal with the intermediate level of interference are summarized in Table 2-2.

The effects of seal wear on h_o as a function of ring interference δ_r is given in Figure 2-24. For the above case of δ_r = 0.5 mm, the 6.5 μm film thickness would upon wear increase to 7.8 μm.

Although interference pressures, film thicknesses, and flow rates can be calculated based on the curves presented herein, a computer program PLGRAD has been provided for calculating these quantities for both worn and unworn seals. The program together with a sample input and output are provided the Appendix to this report.

Table 2-1

Conditions for Numerical Example

Outside Diameter of Seal, D_o,	18.00 mm
Inside Diameter of Seal, D_i,	14.85 mm
Shaft Diameter, D_s,	15.00 mm
Viscosity, μ	55 cps
Elastic Modulus, E,	1.72375 GPa (0.25×10^6 psi)
Speed, N,	4000 rpm
Poissons Ratio, ν	0.46
Stroke, S	34.00 mm
Shaft Radius, $R_s = (D_o + D_i)/4$	8.2125 mm
Seal Thickness, $t = (D_o - D_i)/2$	1.575 mm
Shaft Interference, $\delta_s = (D_s - D_l)/2$	0.075 mm
Shaft Pressure, $p_s = Et\delta/R^2$	3,019 MPa (440 psi)
Diffusion Length $\ell_e = \sqrt{Rt}/[12(1 - \nu^2)]^{1/4}$	2.051 mm

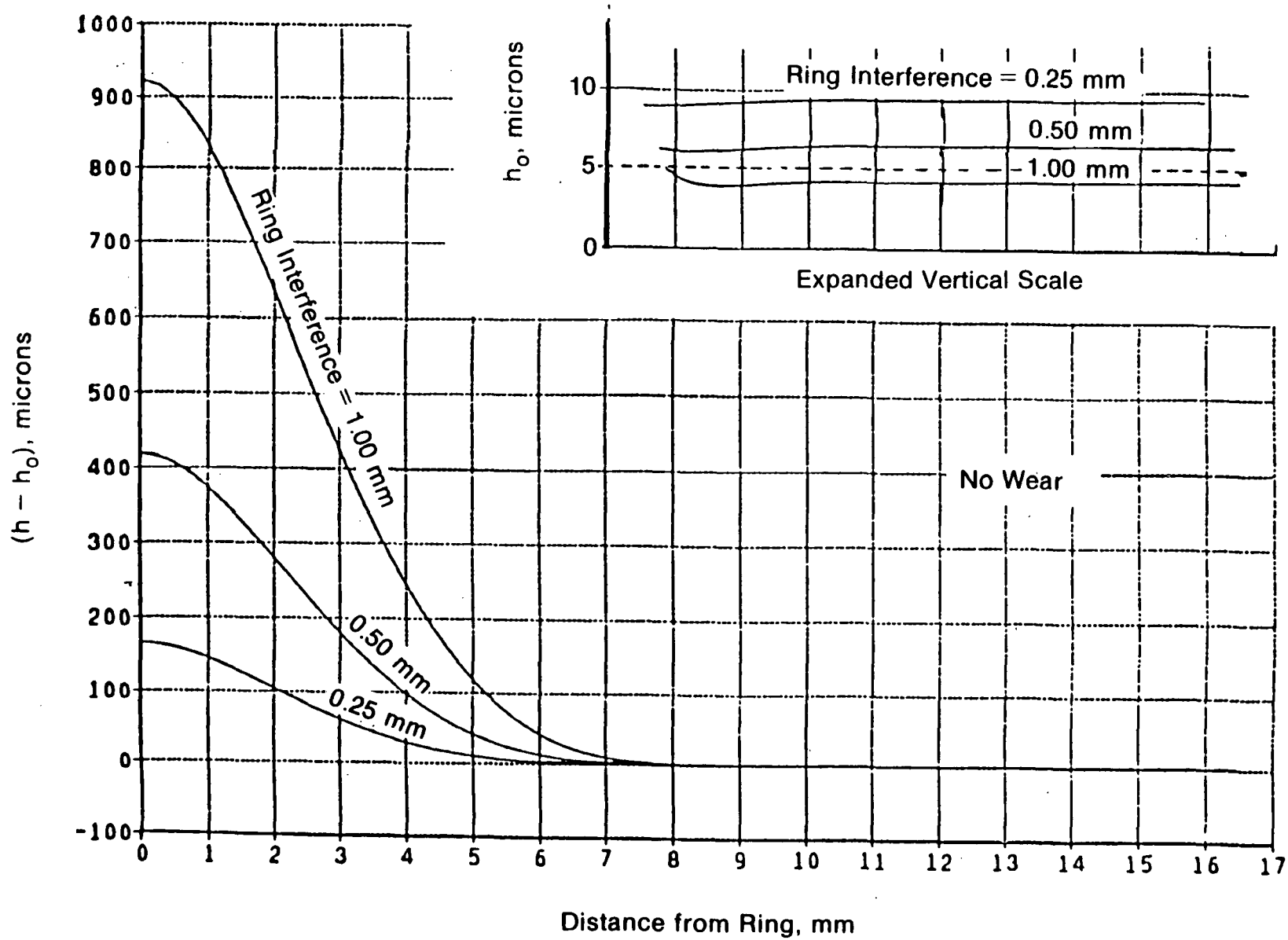

Fig. 2-22 Film Shapes for Ring-Generated Inlets

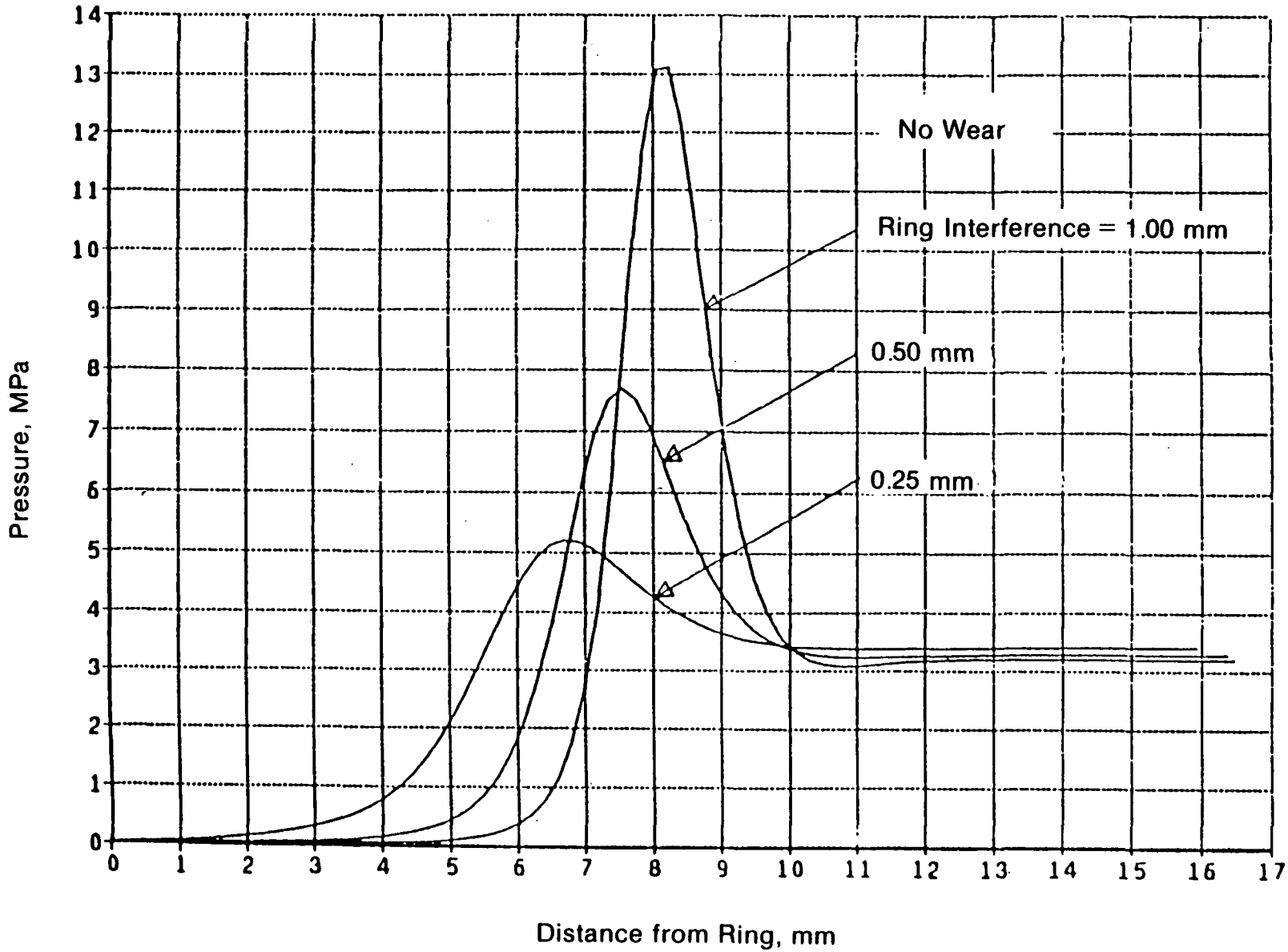

Fig. 2-23 Pressure Profiles for Ring-Generated Inlets

Table 2-2

Results of Numerical Example

Item	SI Units	English Units
Ring Interference	0.5 mm	20 10^{-3} in.
Extent at Lift-Off	7 mm	0.28 in.
Extent at Hydrodynamic Pressures	10 mm	0.40 in.
Peak Pressure Location	7.5 mm	0.30 in.
Peak Pressure	7.7 MPa	1132 psi
Height of h_o	6.5 μm	0.28 10^{-3} in.
Hoop Pressure, p_o	3.2 MPa	470 16 psi

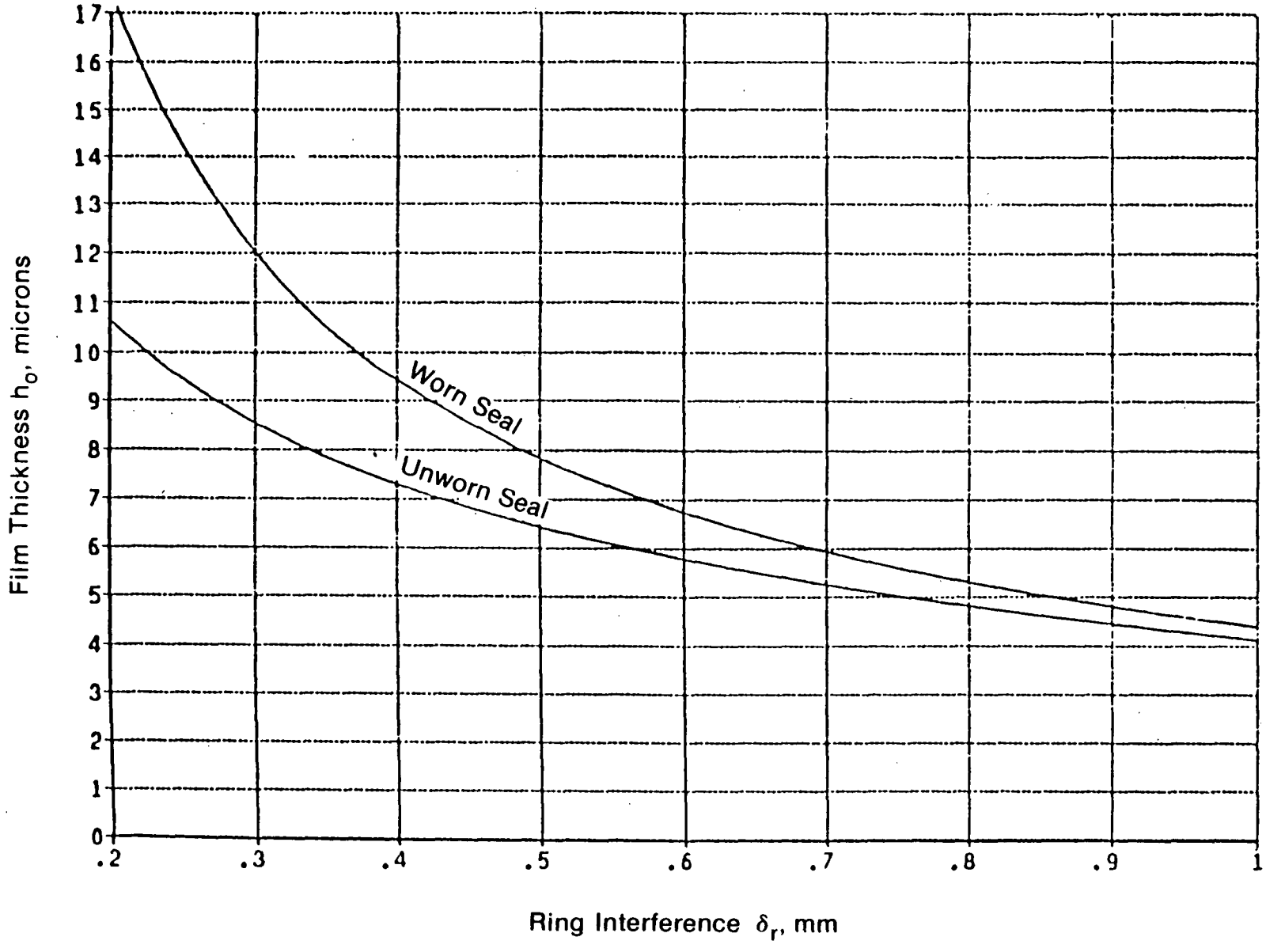

Fig. 2-24 Downstream Film Thickness for Example of Table 1

3.0 EXPERIMENTAL PROGRAM

The analytical treatment of ring-expanded pumping Leningrader (PL) seals provided direction to the task of designing actual functioning seals. An experimental testing program was then developed to provide data for the validation of the analysis and to assess the ring-expanded PL seals performance as a working gas seal.

The experimental test program was divided into two segments. The first, called the "flooded" series, tested PL seals in a total oil environment where oil at a slightly positive head was supplied to what is normally the gas side of the seal. The purpose of the flooded tests was to evaluate the oil pumping capabilities of the PL seal and to assist in the confirmation of the analytical prediction for pumping rates and by inference to the film thickness predictions.

The second test series, referred to as the "gas" tests, evaluated the PL seals in an engine simulation environment with high-pressure gas on one side of the test seal and low pressure "crackcase" oil on the other. The results of these experiments, along with a description of the test apparatus, are discussed in the following sections.

3.1 Test Apparatus

The PL seal experimental program was carried out on reciprocating test apparatus previously employed to evaluate hydrodynamic pumping rings (Ref. 1 and 2). The construction of the apparatus is modular and as such was readily modified to permit testing of pumping Leningrader seals.

The test apparatus, designed and constructed to meet the requirements of this program, provides the following parameters:

Rod Diameter:	19.0 mm
Rod Stroke:	38.1 mm and 50.8 mm
Rotational Speed:	Variable over the range $10 \leq N \leq 60$ Hz

Low-Pressure Oil Supply: 20W40 Oil at pressures to 0.41 MPa
High-Pressure Gas Supply: He at pressures to 10.3 MPa

The lower section of the apparatus contains the cranking mechanism illustrated in Figure 3-1. The crankcase assembly contains a crankshaft (1) that is supported on a pair of automotive-type sleeve bearings (2). An oil seal (3) is provided at the point where the crankshaft penetrates the crankcase for connection to a driver. The crankcase is split horizontally to allow for changing crankshafts. Removable counterweights (4) permit balancing of the crankshaft when changing either the reciprocating mass or the crank throw.

The crankshaft assembly is bolted to a separate base that contains a variable-speed electric motor. A gear tooth belt connects the drive motor to the crankshaft. Isolation mounts are attached underneath the base to provide vibration isolation.

The test head components of the tester are directly connected to the crankcase. These components are identified on the assembly illustrated in Figure 3-2. In this apparatus, a crosshead (1), driven by a connecting rod (2), applies reciprocating motion to the test rod (3). The crosshead is guided as it reciprocates by a crosshead sleeve (4). A lower housing (5), which serves as a foundation for the remainder of the apparatus, includes a manifolding system for providing oil to the crosshead sleeve.

The upper end of the crosshead (1) contains a female taper, which is matched to the taper ground on the end of the test rod (3). Although the taper is sized for locking, a retaining clip (6) is also provided to assure that no relative axial motion exists between the crosshead and the test rod during tester operation.

Mounted directly on the lower housing is a lower guide bearing housing (7), which is designed with a tight piloting arrangement to provide radial positioning. The guide bearing (8) is an externally pressurized, pocketed design, which is supplied with the same oil as the crankcase, thereby eliminating the need for special seals. The oil supply to the guide bearing is adjustable to provide hydraulic shimming of the test rod for alignment purposes. Addi-

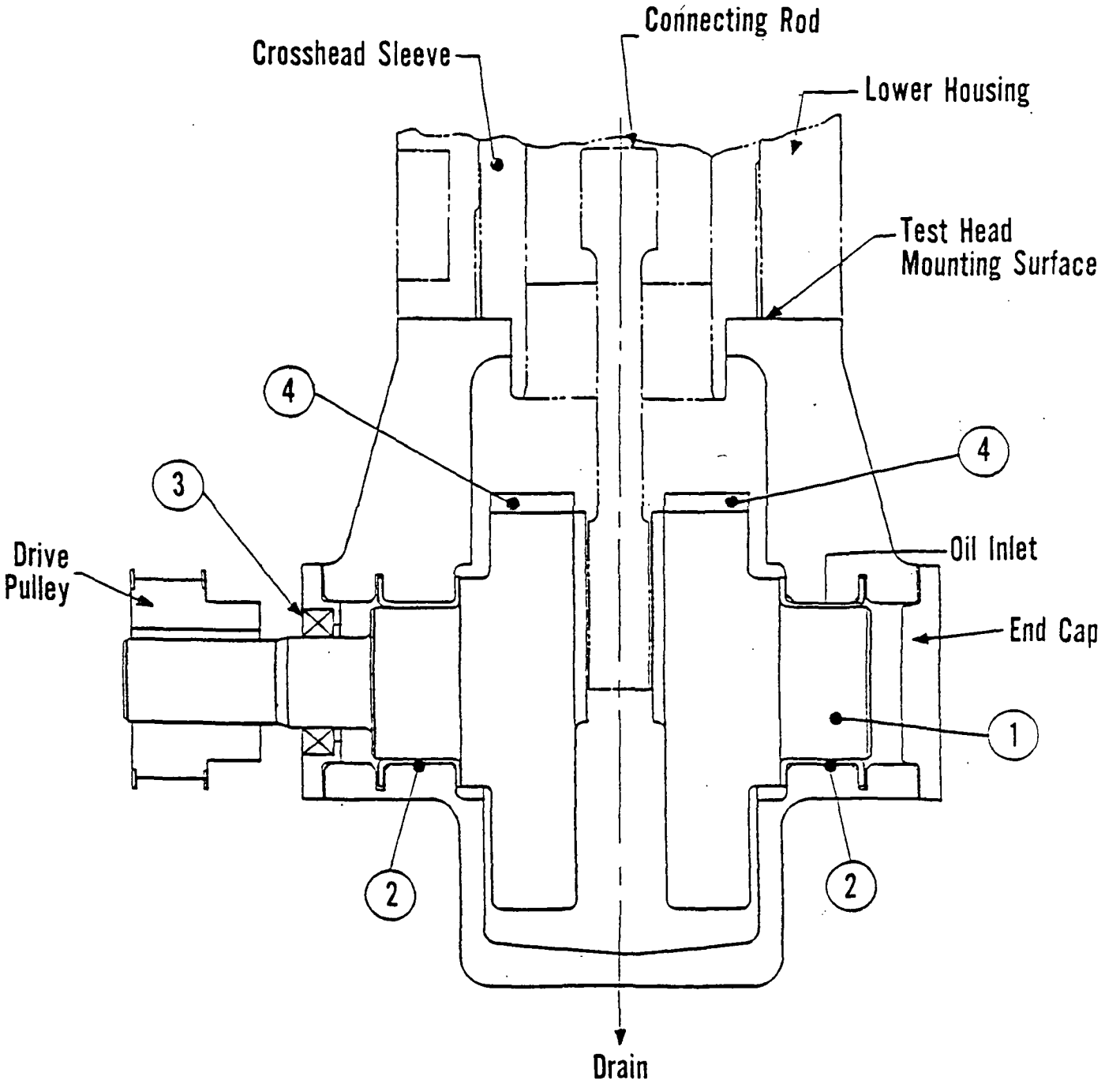

Fig. 3-1 PL Seal Cranking Mechanism

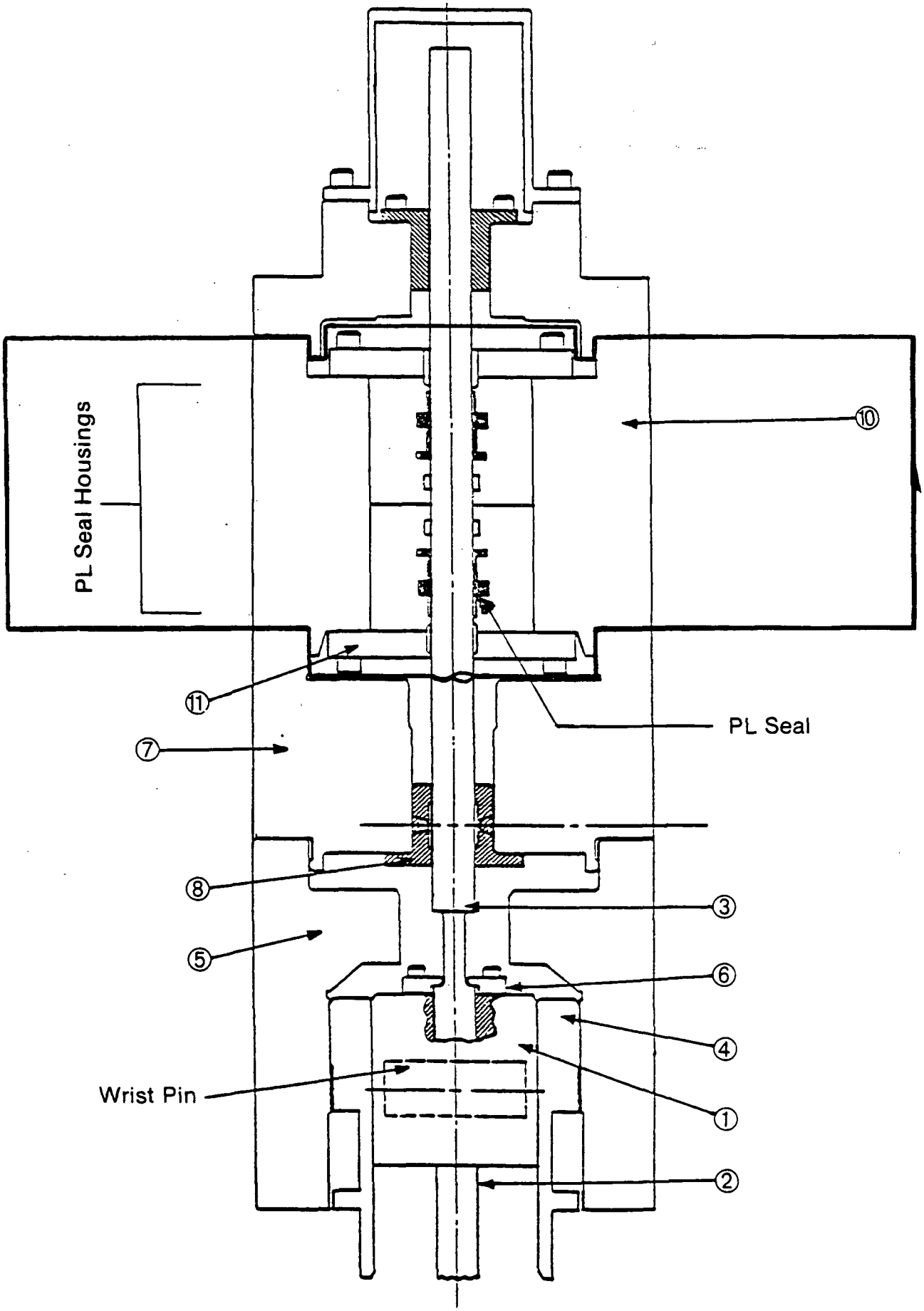

Fig. 3-2 Test Head Assembly

tionally, the guide bearing functions to provide rod cooling which results from the oil exiting the bearing; this design eliminates the need for any auxiliary cooling systems.

Tightly piloted and firmly attached to the lower guide bearing housing are two PL seal housings. A second bearing housing (9) containing a guide bearing (8) is tightly piloted to the upper PL seal housing to ensure proper bearing alignment. A simple cap (10) closes this upper bearing housing.

The two housings and the PL seal installation is shown in Figure 3-3. For this configuration, two seals (1) oriented to pump oil away from each other are tested simultaneously. When fully assembled, the test rod (2) passes through the housing halves (3) which hold the seals (1) and act as a pressure vessel for the liquid or gas to be contained by the seals. Secondary seal seats (4) with integral O-rings and the seal loading sleeves (5) provide the secondary seals for the PL test seals. Springs (6) provide an axial load to seat the seals. The thickness of shims (7) is adjusted to provide a range of preselectable axial loads on the seal. The separating plate (8) allows assembly of the housing halves with the seals installed. Outboard of each seal, annular grooves (9) in the housings supply oil for rod cooling and seal lubrication. Oil drains (10) empty the oil leakage gas separation cavity (11). PTFE inserts (12) maintain a close running gap for leakage containment without the possibilities of rod damage.

For tests under flooded conditions, performed to corroborate analytical predictions, oil at a positive head was supplied to the cavity between the two test seals in the area which is normally exposed to pressurized gas. For starved tests, high-pressure gas rather than oil was introduced into the same cavity so that the seals could be tested at conditions similar to those of rod seals in Stirling engines.

Referring again to Figure 3-3, pressurized gas for gas sealing tests was introduced to the cavity at the center of the housing halves (3). During testing, any leakage gas (13) was flushed out of the separator cavity (11) by the introduction of a known amount of nitrogen gas. Any oil leakage was removed from the seal cavity through flushing ports (14).

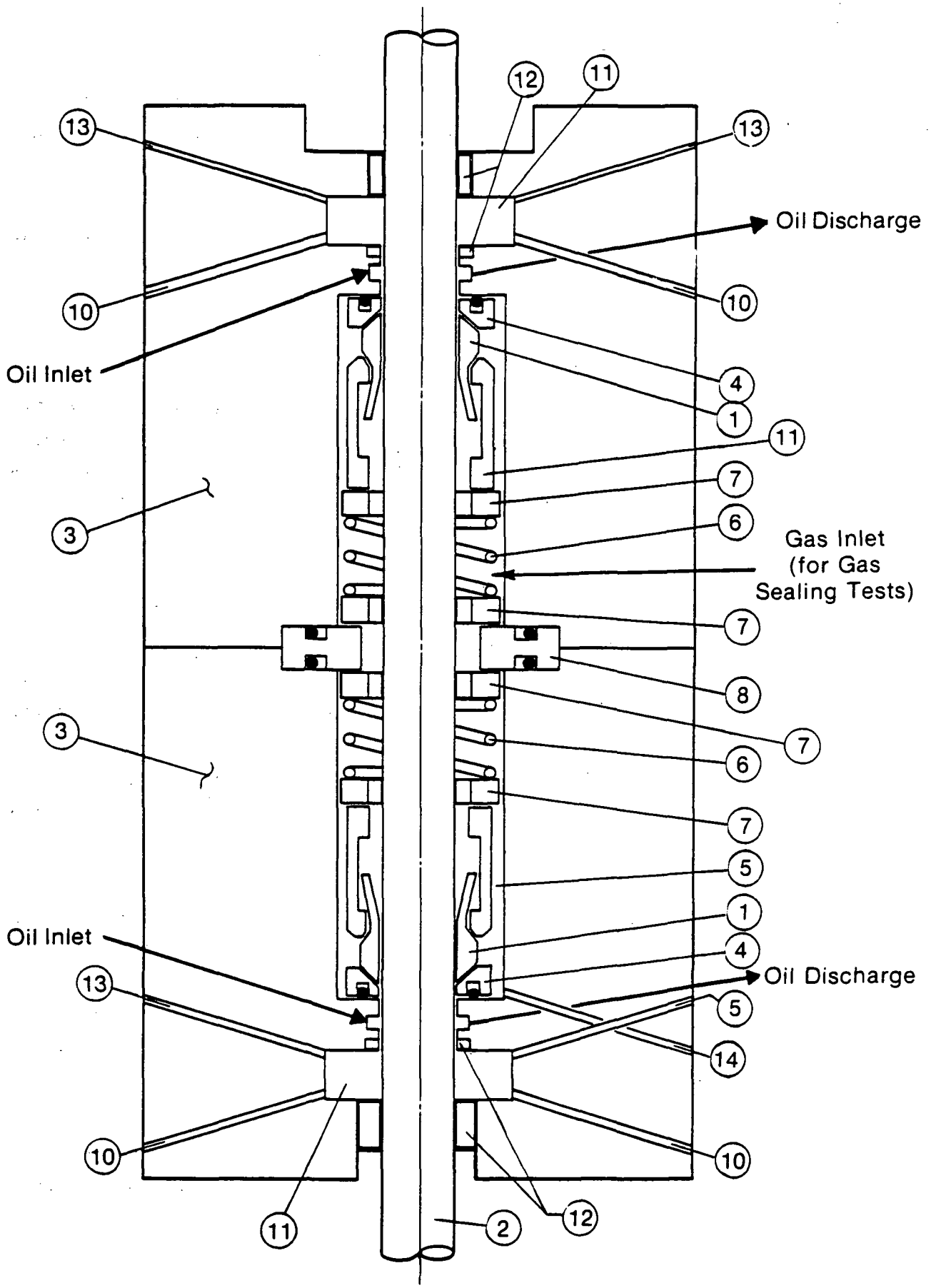

Fig. 3-3 PL Seal Installation

3.2 Material Selection

Material selection for the fabrication of PL test seals was based primarily on the need for candidate materials possessing low elastic modulus values. This requirement was necessary in order to permit reasonable manufacturing tolerances on the seal bore diameter, the diameter which determines the interference fit between the seal and test rod. A second selection criterion was that the seal materials exhibit a resistance to cold flow and provide good dimensional stability.

The final materials selected for PL test seals are listed in Table 3-1. The initial test material choice did not include the PTFE compound since that material had been extensively tested during related programs. Unsatisfactory test results on some of the primary materials, to be described in later report sections, led to inclusion of this material in the final test matrix.

From the many available compounds, the materials indicated on Table 3-1 represent a good variation in flexural modulus coupled with what was felt to be important secondary considerations including low friction coefficients, good dimensional stability (other than the PTFE compounds), and reasonable resistance to deterioration in an environment which could reach 125°C.

3.3 Test Seal Geometry

The design restriction placed on the PL seal geometry was to achieve minimum stress levels while maintaining both sufficient rod interference for proper pumping capacity and adequate expansion ring interference to promote a good inlet geometry, while meeting the maximum envelope restrictions imposed by the test vehicle. The result of these design requirements produced the PL seal envelope geometry illustrated by Figure 3-4. Table 3-2 lists the final seal bore dimensions and the actual interference values under which the seals were tested.

The inlet geometry of the test seals is generated by the expansion of the seal body resulting from the expansion ring interference. Profilometer traces of

Table 3-1

Pumping Leningrader Seal Material Selection

Base Material	Additives	Manufacturer and Trade Name	Elastic Modulus
Modified Phenylene Oxide	Unfilled	General Electric Noryl SE-1	2.48×10^3 MPa
Polyetherimide	Unfilled	General Electric Ultem 1000	3.00×10^3 MPa
Poly(amide-imide)	Unfilled	Amoco Chemicals Torlon 4203	4.58×10^3 MPa
PTFE	Polyimide Powder	Dixon Rulon J	1.59×10^3 MPa

Measurements are in mm unless otherwise specified

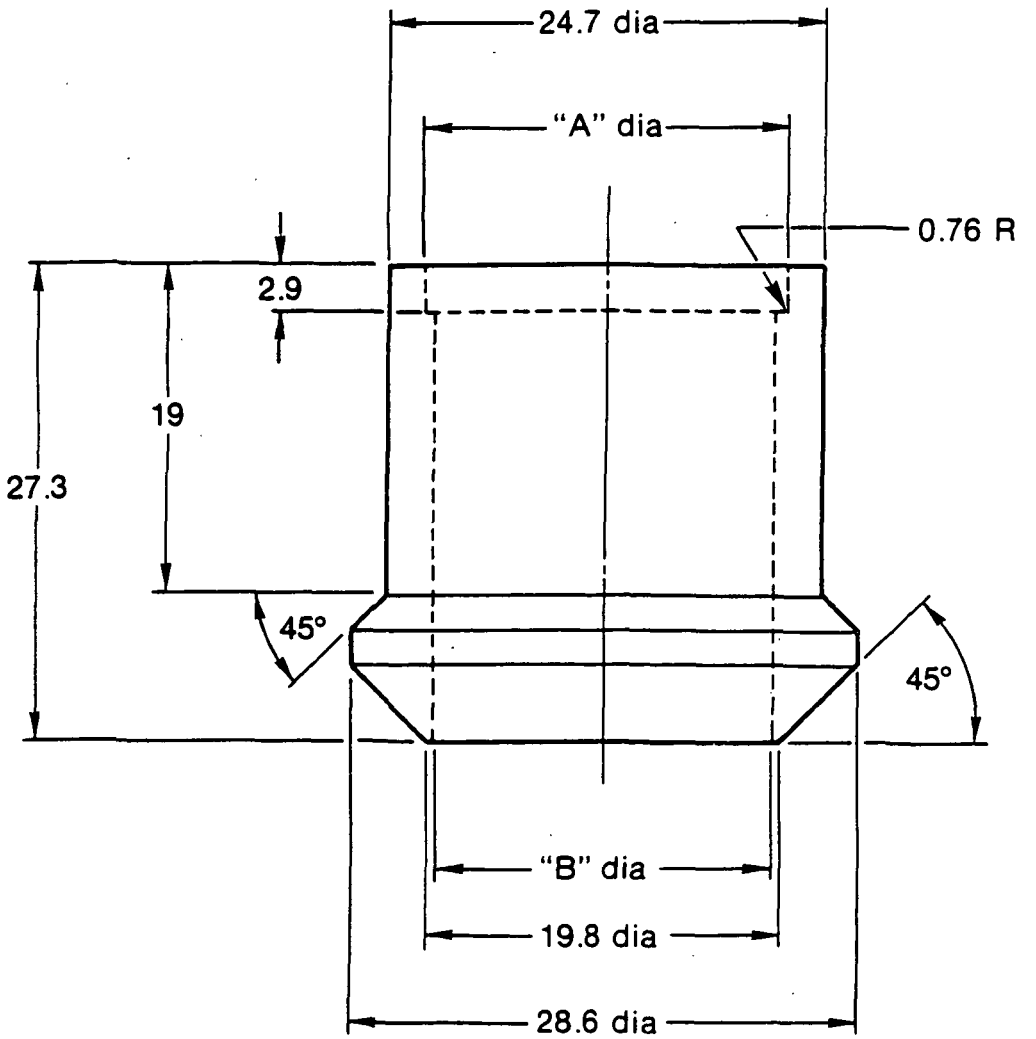

"A" dia = Seat for Ring Expander
"B" dia = Bore for Rod Interference

Fig. 3-4 Pumping Leningrader Seal Geometry

Table 3-2

Test Seal Interferences

•Shaft Diameter: 19 mm nominal
•Ring Expander Diameter: 20.6 mm nominal

Seal Material	Diametral* Shaft Interference 10^{-6} m	Diametral* Ring Expander 10^{-6} m
Modified Phenylene Oxide	45.8 and 53.3	206 and 211
Polyetherimide	50.8 and 48.3	211 and 206
Poly(amide-imide)	50.8 and 48.3	208 and 208
PTFE	140 and 137	328 and 333

*1st number is for upper test seal; 2nd number is for lower test seal

the deflected inlet shape of the seals prior to testing are reproduced on Figure 3-5. The illustrated contours agree with predicted shapes.

3.4 Test Method and Results

The objective of the pumping Leningrader seal test program was to evaluate the performance of several seal designs over a range of operating conditions as a means of validating the advanced seal analysis. The fixed parameters under which the seals were tested include:

- Oil Type: 20W40
- Gas Type: He
- Inlet Oil Temp: 49°C
- Reciprocating Stroke: 38.1 and 50.8 mm
- Rotational Frequency: 10, 35, 60 Hz

Two test sequences were employed for experimentally verifying the PL seal analysis. Test Sequence 1, the "flooded" test in which oil at a positive pressure was supplied to the inlet of the test seals, was intended to provide the necessary data for correlation with analytically predicted flow characteristics. Test Sequence 2, the "gas" tests in which the test seals were evaluated in a more realistic environment with high-pressure gas, was intended as a verification of the ring-expanded PL seal design as a capable reciprocating gas seal.

Each of the two test sequences were evaluated under their own unique test conditions which included:

- For "flooded" tests
  - oil inlet pressures of 0.21 and 0.41 MPa
  - oil discharge pressure of 0+ mm Hg
  - all seal materials tested at 50.8 mm stroke
  - one material tested at 25.4 mm stroke
- For "gas" tests
  - gas inlet pressures of 10.3 and 5.2 MPa
  - oil discharge pressures of 0+ mm Hg and 0.069 Mpa

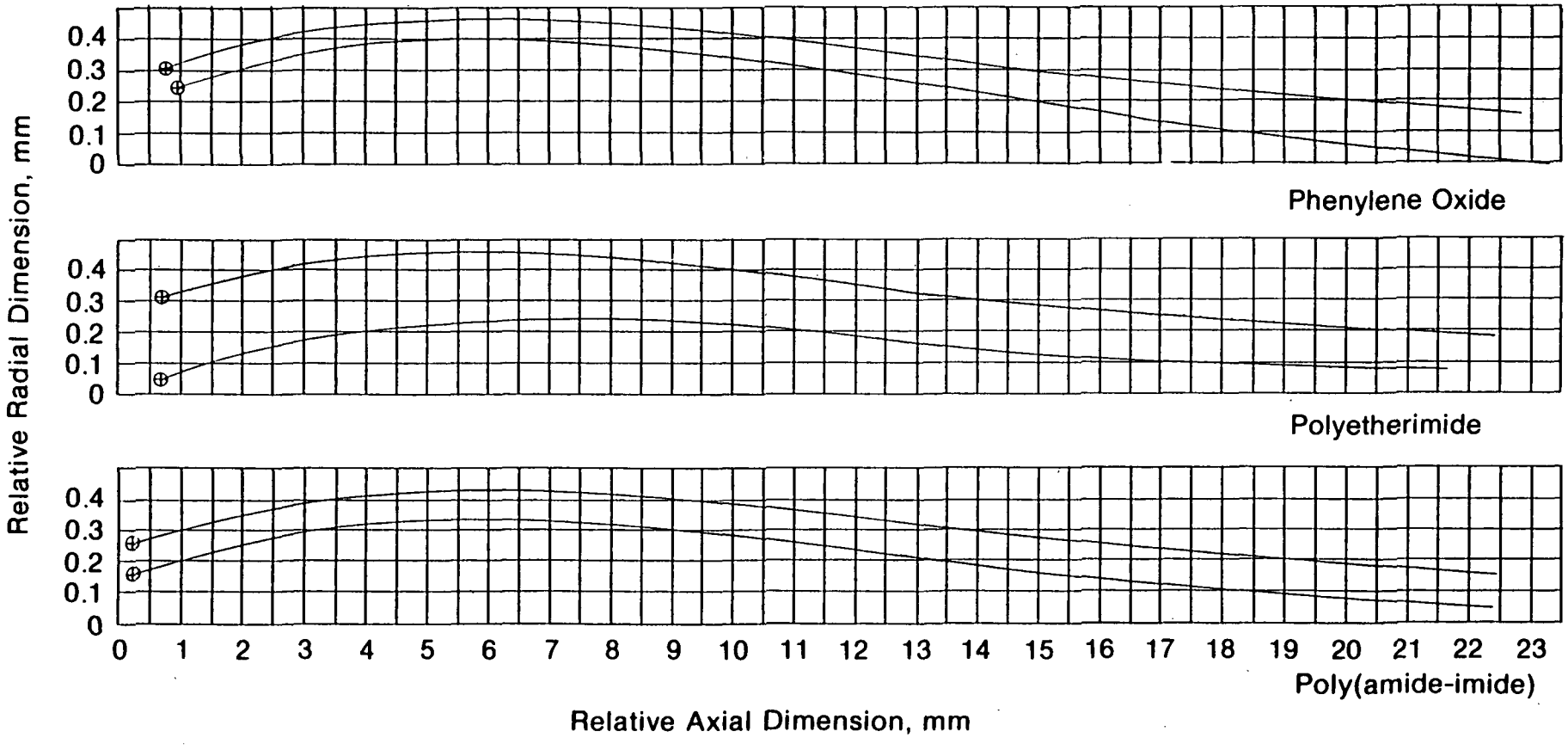

Fig. 3-5 Pretest Inlet Geometry

Prior to actual seal testing, the level of preload exerted on the test seals by the preload springs was established. The proper seal load is achieved by adjustment of the shims controlling seal spring compression (Item 6 of Figure 3-3). The shims were adjusted to provide a 365-N spring load for all the seal tests reported. This level of preload is sufficient to maintain secondary seal compression both for start-up conditions and for flooded tests. The high pressure exerted on the seals during gas sealing tests provided additional secondary seal loads.

3.4.1 Flooded Tests

The three primary materials were tested for pumping capability at the long stroke of 50.8 mm. The results of these tests are presented in Tables 3-3, 3-4, and 3-5 for the modified phenylene oxide, the polyetherimide, and the poly(amide-imide), respectively. Recorded on these tables is the test rod reciprocating frequency, oil inlet pressure and temperature, seal temperatures, and the delivered flow (sum of two seals).

Data points at the specified rod speeds reflect data taken over a long period of time. To assist in viewing these data for performance trends, the mean temperature levels and flow rates for each speed and inlet pressure combination were examined. Although the variance of each mean temperature may appear excessive, these means, as presented in Table 3-6, do indicate trends not entirely evident when viewing the nonaveraged data.

Just prior to the conclusion of the long-stroke tests on the modified phenylene oxide test seals, erratic flow behavior was noted. Examination of both test seals revealed longitudinal cracks had occurred in the thin wall sections extending from the expansion ring to the start of the trapezoidal cross section. Since the seals had already been designed to provide minimum stress levels for the available envelope restrictions, it was concluded that testing of the modified phenylene oxide in its present configuration should be discontinued.

A replacement material of PTFE with a polymer powder additive was selected for gas seal testing so that a three-material test matrix could be maintained.

Table 3-3

Flooded Test Results - Modified Phenylene Oxide

Stroke 50.8 mm, Oil = 20W40 (Mobil Delvac)

Speed cpm	Inlet P MPa	Inlet T °C	Temp. °C(1)	Temp. °C(2)	Flow cc/min	(Average)
10	0.21	30	48	49	420	
10	0.21	29	48	48	429	(426)
10	0.21	29	47	47	429	
10	0.41	30	53	54	411	
10	0.41	30	51	52	438	(432)
10	0.41	31	49	49	447	
35	0.21	26	48	46	742	
35	0.21	28	54	54	742	(739)
35	0.21	31	59	53	733	
35	0.41	29	114	52	769	
35	0.41	30	59	59	733	(748)
35	0.51	31	60	60	742	
60	0.21	29	52	52	1317	
60	0.21	34	64	63	1218	(1251)
60	0.21	37	69	68	1218	
60	0.41	37	75	71	1152	
60	0.41	38	75	72	1053	(1075)
60	0.41	38	77	73	1020	

(1) Upper Seal
(2) Lower Seal

Table 3-4

Flooded Test Results - Polyetherimide

Stroke 50.8 mm, Oil = 20W40 (Mobil Delvac)

Speed Hz	Inlet P MPa	Inlet T °C	Temp. °C(1)	Temp. °C(2)	Flow cc/min	(Average)
10	0.21	28	47	45	250	
10	0.21	28	48	48	277	(271)
10	0.21	28	48	47	286	
10	0.41	29	58	56	260	
10	0.41	29	53	55	259	(262)
10	0.41	29	53	52	268	
10	0.41	29	52	50	259	
35	0.21	28	52	52	465	
35	0.21	28	56	53	554	(521)
35	0.21	28	60	58	545	
35	0.21	26	43	43	554	
35	0.21	27	49	51	572	(560)
35	0.21	28	58	60	554	
35	0.41	28	61	63	554	
35	0.41	28	64	67	554	(554)
60	0.21	28	60	64	751	
60	0.21	29	76	77	662	(694)
60	0.21	29	79	80	670	
60	0.41	29	83	84	670	
60	0.41	29	87	87	670	(672)
60	0.41	29	89	88	679	
60	0.41	30	89	86	670	

(1) Upper Seal
(2) Lower Seal

Table 3-5

Flooded Test Results - Poly(amide-imide)
Stroke 50.8 mm, Oil = 20W40 (Mobile Delvac)

Speed Hz	Inlet P MPa	Inlet T.°C	Temp. °C(1)	Temp °C(2)	Flow cc/min
10	0.21	28	48	49	322
10	0.21	29	49	50	331
10	0.21	29	50	51	322
10	0.41	30	64	66	304
10	0.41	30	60	62	313
10	0.41	30	45	58	304
35	0.21	26	47	42	626
35	0.21	27	60	81	608
35	0.21	28	66	67	608
35	0.41	28	69	68	617
35	0.41	29	72	70	608
35	0.41	29	73	72	617
60	0.21	29	68	66	769
60	0.21	30	79	76	706
60	0.21	30	85	82	688
60	0.42	31	86	83	679
60	0.42	32	89	87	670
60	0.42	32	90	89	688

(1) Upper Seal
(2) Lower Seal

Table 3-6

Mean Temperature Levels and Flow Rates

Seal Material	N Hz	P MPa	T_{mean} °C	ΔT °C	Flow cc/min
Modified Phenylene Oxide (Noryl)	10	0.21	48/48	18/18	426
	35	0.21	54/51	26/23	739
	60	0.21	62/61	28/28	1251
	10	0.41	51/52	21/22	432
	35	0.41	58/57	28/27	748
	60	0.41	76/72	39/36	1075
Polyetherimide (Ultem)	10	0.21	47/47	19/18	271
	35	0.21	50/51	23/24	560
	60	0.21	72/74	43/45	694
	10	0.41	54/53	24/24	261
	35	0.41	63/65	35/37	554
	60	0.41	87/86	58/57	672
Poly(amide-imide) (Torlon)	10	0.21	49/50	20/22	325
	35	0.21	57/56	30/28	614
	60	0.21	78/74	48/45	721
	10	0.41	60/62	30/32	307
	35	0.41	71/70	43/42	614
	60	0.41	88/86	57/54	679

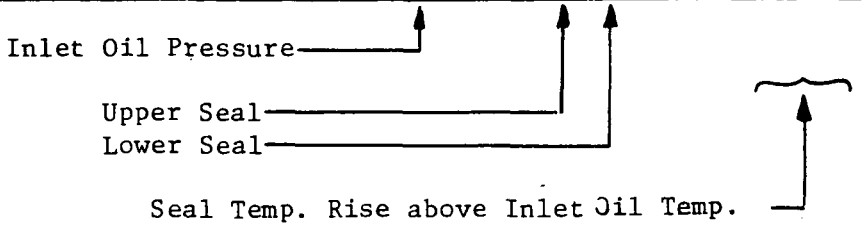

A short-stroke (25.4 mm) test was run using the polyetherimide seals. At this stroke, which was less than the overall length of the seals themselves, oil pumping occurred only at maximum conditions of speed and inlet oil pressure and then only as miniscule amounts. After several unsuccessful attempts to improve the flow rates, the short-stroke tests were terminated.

3.4.2 Gas Sealing Tests

At the conclusion of the flooded tests, the apparatus was refitted for gas sealing tests. At the same time the new set of PTFE seals was inspected for rod and expansion ring interference. Because of the known tendency for PTFE to exhibit permanent dimensional changes when under stress, the nominal interference levels were increased above that of the other seals.

The rod interferences for the PTFE seals were measured at 140 and 136 x 10^{-6} m for seals 1 and 2, respectively. The expansion ring interferences for the same seals were 328 and 332 x 10^{-6} m.

The flooded tests had confirmed the high forward stroke pumping capability of the ring-expanded seals. It was important for the gas test however to assure that some oil for seal lubrication would be brought into the seal-rod interface on the return stroke. The oil entering the gas side of the seal would then be removed by the strong pumping action of the ring-expanded seal's geometry.

To provide a weak but otherwise effective pumping action on the return stroke, each test seal was provided with a small inlet chamfer as illustrated by Figure 3-6.

Actual chamfer dimensions were confirmed by profilometer trace measurements and are shown in Table 3-7.

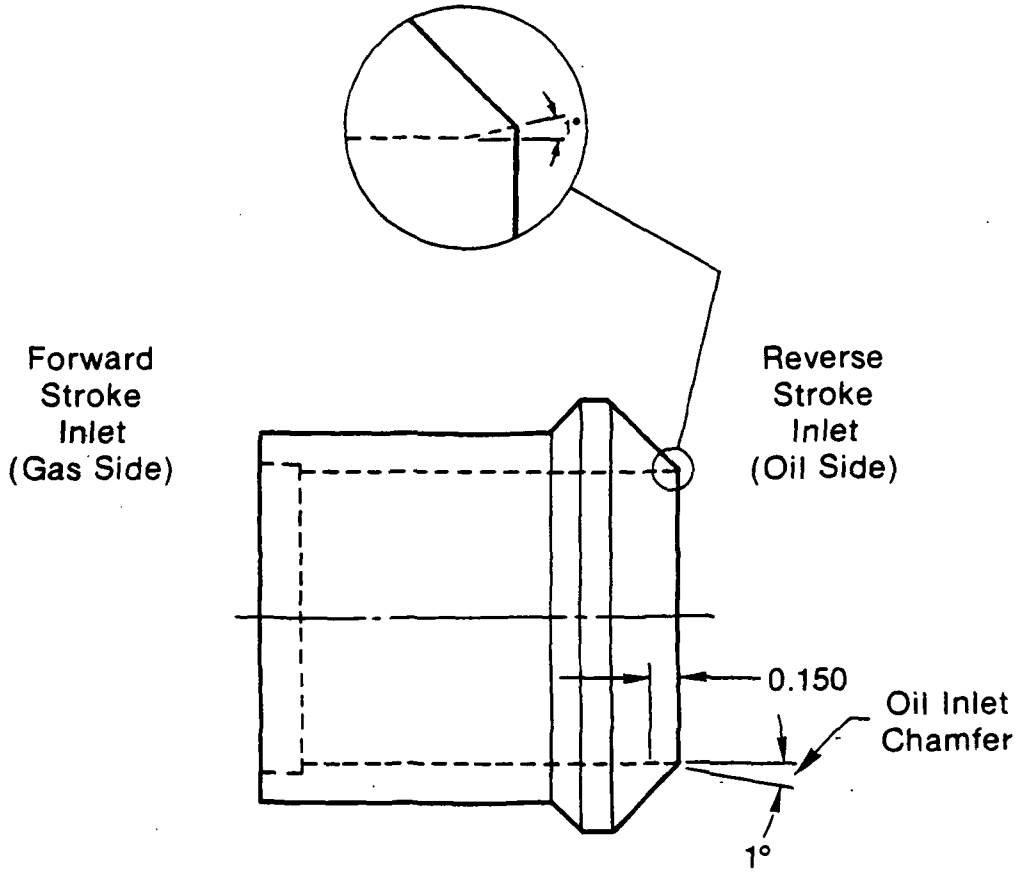

Fig. 3-6 Test Seal with Small Inlet Chamfer

Table 3-7

Return Stroke Inlet Chamfer Geometry

Seal Material	Chamfer <	Chamfer Extent
Polyetherimide	0° - 31'	0.145
Poly(amide-imide)	0° - 35'	0.148
PTFE	1° - 02'	0.150

Gas sealing tests were conducted for various combinations of gas pressure, oil inlet pressure, and reciprocating frequency at one stroke. For comparison purposes, one set of test conditions was run at a shorter stroke. The following list indicates the values of the parameters actually tested:

Gas Pressure:	5.2 and 10.3 MPa
Oil Pressure:	0+ and 0.07 MPa
Reciprocating Frequency:	16.7, 30.0, 60.0 Hz.
Stroke:	50.8 mm primary, 38.1 mm secondary

The three seal materials were tested at all combinations of pressure (both gas and oil) and frequency. For each combination of test conditions, the seals were run until temperature stabilization occurred, at which time any gas leakage was measured and the seal temperatures recorded. To end each test cycle, a mid-speed and lower gas pressure combination was run for several hours.

At the completion of each test point the tester was disassembled and oil wetted parts in the gas side of the seal were examined and any residual oil weighed.

The results for the poly(amide-imide) seal tests are given on Tables 3-8 and 3-9, the polyetherimide seal tests on Tables 3-10 and 3-11, and the PTFE seal tests on Tables 3-12, 3-13, and 3-14.

Table 3-8

Poly(amide-imide) Gas Seal Test Results

(Oil Leakage - Average for Run 0.51 g/hr; Total Run Time 3:30)
(Stroke 50.8 mm; Oil Side Pressure 0+)

Gas Side Pressure MPa	Reciprocating Frequency Hz	Upper Seal Leakage Rate cc/min	Lower Seal Leakage Rate cc/min	Oil Inlet Temp °C	Upper Seal Temp °C	Lower Seal Temp °C
5.2	16.7	0.15	0.12	36.8	Thermocouple Inoperative	59.6
5.2	30.0	3.00	0.45	37.7		58.5
5.2	60.0	4.20	4.80	39.8		62.8
10.3	16.7	Off Scale	0.36	42.3		62.8
10.3	30.0	Off Scale	1.50	42.7		65.1
10.3	60.0	1.65	4.80	42.9		66.3
5.2	30.0	0.51/4.50	1.35/4.80	47.6		58.7

Table 3-9

Poly(amide-imide) Gas Seal Test Results

(Oil Leakage - Average for Run 0.3 g/hr; Total Run Time 4:00)
(Stroke 50.8 mm; Oil Side Pressure 0.07 MPa)

Gas Side Pressure MPa	Reciprocating Frequency Hz	Upper Seal Leakage Rate cc/min	Lower Seal Leakage Rate cc/min	Oil Inlet Temp °C	Upper Seal Temp °C	Lower Seal Temp °C
5.2	16.7	2.40	0.26	27.0		59.6
5.2	30.0	0.30	1.05	30.6	Thermocouple Inoperative	38.9
5.2	60.0	Off Scale	3.30	31.6		44.3
10.3	16.7	Off Scale	6.60	38.8		46.9
10.3	30.0	Off Scale	6.30	37.1		48.0
10.3	60.0	Off Scale	6.00	33.4		49.7
5.2	30.0	0.012/ Off Scale	0.03/0.51	34.2		47.8

Table 3-10

Polyetherimide Gas Seal Test Results

(Oil Leakage - Average for Run; Trace; Total Run Time 7:00)
(Stroke 50.8 mm; Oil Side Pressure 0+)

Gas Side Pressure MPa	Reciprocating Frequency Hz	Upper Seal Leakage Rate cc/min	Lower Seal Leakage Rate cc/min	Oil Inlet Temp °C	Upper Seal Temp °C	Lowe Seal Temp °C
5.2	16.7	Off Scale	13.8	47.1	37.1	53.4
5.2	30.0	0.69	0.63	46.7	41.4	56.6
5.2	60.0	Off Scale	5.10	46.5	47.0	70.0
10.3	16.7	19.5	0.63	47.2	40.3	61.1
10.3	30.0	2.55	2.55	47.9	41.2	71.0
10.3	60.0	3.00	7.20	48.8	62.0	74.2
5.2	30.0	0.30/18.0	1.32/2.70	47.8	57.5	68.7

Table 3-11

Polyetherimide Gas Seal Test Results

(Oil Leakage - Average for Run 2 g/hr; Total Run Time 2:18)
(Stroke 50.8 mm; Oil Side Pressure 0.07 MPa)

Gas Side Pressure MPa	Reciprocating Frequency Hz	Upper Seal Leakage Rate cc/min	Lower Seal Leakage Rate cc/min	Oil Inlet Temp °C	Upper Seal Temp °C	Lower Seal Temp °C
5.2	16.7	0.42	1.05	26.9	38.7	50.2
5.2	30.0	0.90	2.70	28.2	41.0	54.0
5.2	60.0	0.45	1.50	35.0	51.4	62.0
10.3	16.7	10.5	1.08	36.2	59.0	65.1
10.3	30.0	10.5	1.20	38.0	64.8	72.9
10.3	60.0	Off Scale	3.00	39.4	69.6	80.8
5.2	30.0	0.09/12.6	0.27/0.81	47.2	58.8	67.1

Table 3-12

PTFE Gas Seal Test Results

(Oil Leakage - Average for Run 0.34 g/hr; Total Run Time 5:00)
(Stroke 50.8 mm; Oil Side Pressure 0+)

Gas Side Pressure MPa	Reciprocating Frequency Hz	Upper Seal Leakage Rate cc/min	Lower Seal Leakage Rate cc/min	Oil Inlet Temp °C	Upper Seal Temp °C	Lower Seal Temp °C
5.2	16.7	0.33	0.27	35.9	30.8	39.7
5.2	30.0	2.70	0.45	37.3	34.6	46.2
5.2	60.0	2.40	3.30	39.1	43.1	59.6
10.3	16.7	0.45	0.72	42.3	42.7	56.3
10.3	30.0	2.40	0.54	41.5	42.3	58.4
10.3	60.0	2.40	2.70	39.7	41.8	66.0
5.2	30.0	0.12/3.00	0.42/2.70	48.9	46.3	62.5

Table 3-13

PTFE Gas Seal Test Results

(Oil Leakage - Average for Run, Trace; Total Run Time 5:00)
(Stroke 50.8 mm; Oil Side Pressure 0.07 MPa)

Gas Side Pressure MPa	Reciprocating Frequency Hz	Upper Seal Leakage Rate cc/min	Lower Seal Leakage Rate cc/min	Oil Inlet Temp °C	Upper Seal Temp °C	Lower Seal Temp °C
5.2	16.7	0.36	0.10	41.3	33.6	38.4
5.2	30.0	0.22	0.60	42.0	37.0	40.8
5.2	60.0	3.30	3.60	43.8	____	48.2
10.3	16.7	Off Scale	0.09	44.1	____	47.8
10.3	30.0	Off Scale	2.10	43.5	____	49.2
10.3	60.0	0.66	5.70	42.8	____	53.3
5.2	30.0	Off Scale	0.04/6.30	48.6	55.2	55.7

Table 3-14

PTFE Gas Seal Test Results

(Oil Leakage - Average for Run, Trace; Total Run Time 3:30)
(Stroke 38.1 mm; Oil Side Pressure 0.07 MPa)

Gas Side Pressure MPa	Reciprocating Frequency Hz	Upper Seal Leakage Rate cc/min	Lower Seal Leakage Rate cc/min	Oil Inlet Temp °C	Upper Seal Temp °C	Lower Seal Temp °C
5.2	16.7	0.36	0.10	30.0	30.4	29.1
5.2	30.0	0.06	0.33	33.0	37.0	36.8
5.2	60.0	0.05	0.69	37.8	46.0	50.5
10.3	16.7	0.07	0.54	41.0	46.0	44.2
10.3	30.0	0.02	0.13	41.5	50.0	50.0
10.3	60.0	1.68	0.69	46.3	59.7	60.2
5.2	30.0	0.04/17.1	∿0/1.56	51.6	56.6	57.0
5.2*	16.7	0.09/5.1	2.40/8.70	50.3	53.6	46.6

*Data taken following day

4.0 DISCUSSION OF RESULTS

4.1 Flooded Tests

The purpose of conducting the flooded PL seal tests was to generate actual flow data which could then be used for correlation with analytically predicted performance. The flooded tests confirmed the excellent pumping capability of the expanded-ring inlet geometry of the new PL seal design; an important attribute if the seal is to successfully purge any oil which may enter the gas side of the seal.

To illustrate the degree of correlation between the test data and analytically predicted flow values, each data item listed in Table 3-6, which represents the sum of flow rates for double-acting seals, is presented for comparison purposes with the flow rates calculated using PLGRAD (See Appendix) in Table 4-1.

In several areas, agreement between prediction and test is quite good, with major deviations occurring with underpredictions at 10 Hz and for the highest elastic modulus seal.

The test data is consistent with expected results in that supply pressure has little or no effect on flow rate. There is evidence, as seen in Table 3-6, that flow rates even decrease slightly with increases in supply pressure. This decrease, however, may be more a result of changes in seal loading rather than from other, more obscure reasons.

In addition, there seems to be only a modest effect on flow rates from variations in seal operating temperatures. At each test frequency, data were collected over an extended period of operational time in order to monitor seal temperature stabilization. The effect on flow of an increasing seal temperature during an otherwise stable test condition is not zero but is definitely a minor consideration, at least over the range of temperatures experienced. This minimal effect is evident by the narrow scatter band of pumped flow rates at each fixed speed and inlet pressure.

Table 4-1

Experimental and Analytical Flow Rate Comparison
Flooded Tests

Seal Material	Inlet P MPa	N Hz	Tmean °C	Flow Rate cc/min Experiment	Flow Rate cc/min Analysis
Modified		10	48/48	426	64.2
Phenylene Oxide	0.21	35	54/51	739	656.0
		60	62/61	1251	1356.0
(Noryl)	--	10	51/52	432	57.1
	0.41	35	58/57	748	549.0
		60	76/72	1075	942.0
Polyetherimide		10	47/47	271	49.8
	0.21	35	50/51	560	489.0
(Ultem)	--	60	72/74	694	858.0
		10	54/53	261	44.4
	0.41	35	63/65	554	382.0
		60	87/86	672	743.0
Poly(amide-imide)		10	49/50	325	20.9
	0.21	35	57/56	614	200.0
(Torlon)	--	60	78/74	721	364.0
		10	60/62	307	13.6
	0.41	35	71/70	614	132.0
		60	88/86	679	245.0

There are two other parameters affecting pumped flow rates. One is the obvious speed dependent effect, and the other, a more subtle effect resulting from material properties.

As speeds were increased above the first test speed of 10 Hz, a rapid rise in pumped flow rate was experienced. As the maximum test speed of 60 Hz was approached, however, the rate of oil pumping seemed to be approaching a maximum. The material effect is demonstrated by the much higher pumping flow rate exhibited by the Phenylene Oxide seals with lower flow rates produced by the higher modulus material.

The speed effect is affected by two processes acting in concert. As reciprocating rod velocities are increased, more fluid per unit time can enter the seal inlet to generate higher film pressures and a larger film thickness, thereby producing an increased flow rate. At the same time, however, at the transition between the forward and rearward rod velocity directions, the elasticity of the seal must collapse the fluid film in order to shut off any reverse flow. At very low speeds the oil volume brought into the inlet is low and the time available to collapse the fluid film by squeeze-film effects is high, thereby providing a low flow rate with minimal backflow. At moderate speeds the volume of oil brought into the seal is increased but some backflow exists since the fluid squeeze film collapse time is now a larger percentage of the stroke period. At higher speeds, although the volume of oil introduced into the seal is large, the squeeze film collapse time is now a significant portion of the cycle time, and backflow flow rates can be a significant portion of incoming rates; the net result being a leveling off of the pumped flow rates.

The effect of PL seal material elastic modulus on the rate at which seals pump is attributed to restrictions to film thickness development caused by higher elastic modulii. Lower values of film thickness produced by higher material stiffness properties would inhibit the development of high flow rates.

Two test results differ significantly from analytical predictions; one is the high flow rates produced by all seals at a speed of 10 Hz, the second is the

higher than predicted flows produced by the poly(amide-imide) seals. Both results may be explained as follows.

At 10 Hz, where sufficient time at the end-of-stroke direction would permit fluid film collapse, the static friction force developed between the seal and the test rod could be sufficient to diminish the effectiveness of the PL seal's outer diameter static seal (Figure 2-1). This loss of sealing capacity could allow oil to by-pass the PL seal and bias its actual performance, thereby producing the results seen. Since the preload spring for the test seals has a very high spring rate (1.74×10^7 N/M), very small seal motions would quickly overcome any static friction force development to limit any lift-off; this, combined with a long drain path for the leakage flow, would provide sufficient flow resistance to prevent an extremely large amount of leakage to occur.

The same arguments can be applied to the test results for the poly(amide-imide) test seals which show a much higher than anticipated flow rate. For this material, because of its higher modulus, sufficiently large friction forces could be developed at all speeds to provide a flow bias for all the test points.

4.2 Gas Sealing Tests

The results of the gas sealing tests for each of the three seal materials show wide variations in gas leakage at essentially similar test conditions. This variability even extends to the long-term tests where independent variables were maintained constant. Greater gas leakage variability does however seem to be associated with the seal materials with high elastic modulus values although even the PTFE seals suffer from this apparent phenomena.

The accuracy of the gas leakage values depends on exactly how the gas (in this case He) which actually leaks past the seal mixes with the purged gas. If the purged gas is not well mixed with the leakage gas at the time of sampling, the helium leak detecting system may record higher proportional levels of helium in the purged gas mixture than are actually present. This problem seems to have occurred with some frequency since it was possible under certain circum-

stances to obtain large differences in detector readings over short time periods at supposedly steady-state operation.

One conclusion which can be readily drawn from the gas tests is that the wide variability in the data taken for each seal requires that large test samples of many seals must be evaluated before a statistically sound judgment of performance can be made.

The evidence is strong that low modulus PL seal materials such as PTFE outperform higher modulus materials such as poly(amide-imide) with respect to both oil and gas leakage. This conclusion is based, however, on single sample test results and may not hold up under the scrutiny of multiple sample testing.

One good argument for the use of lower modulus materials for the construction of PL seals is the freedom this material type permits in establishing seal dimensions. Larger seal-to-piston-rod interferences permitted by low elastic modulus materials means than larger tolerance can be applied to the seal bores without concern for substantially lowering the interference contact pressure that would result from the same tolerance applied to stiffer materials.

At the conclusion of the polyethermide test sequence, a visual examination of the test seals revealed that both the upper and lower seals had experienced serious structural failures. These failures manifested themselves as circumferential cracks in the trapezoidal sections of the seals; cracks which extended from the secondary seal surface axial through a portion of the heavy trapezoidal seal section. There is no evidence that these cracks, most likely the result of elevated shear stresses induced by the high sealed gas pressures, projected through the body of the seal to permit leakage of either gas or oil. The fact that the cracks appeared after a relatively short testing period (9 hr 18 min) does not provide confidence for the materials long-term durability.

Of the two remaining materials which did not show distress after testing, the poly(amide-imide) with its very high elastic modulus still presents problems for the PL seal designer. The high modulus of this material requires that its

rod interference be kept small in order to minimize starting friction problems and to alleviate assembly difficulties which would result from forces generated by large interference fits.

The combination of the low interference fit and high elastic modulus of the poly(amide-imide) material also means less conformity of the material to the small irregularities which occur during manufacture. Relative lack of conformability may explain why this particular material showed high leakage of both gas and oil during the sealing tests.

5.0 DISCUSSION AND CONCLUSIONS

The analysis presented in this report is capable of predicting seal performance and sensitivity of the seal performance to wear. The ring-induced inlet appears to have low sensitivity to the wearing-in process and provides excellent pumping capacity and large films.

Experimental work has demonstrated the ring-induced inlet PL seal pumps oil at high flow rates and has the ability to provide excellent sealing capability. Limited seal tests, however, did not permit a rigorous statistical evaluation of seal performance.

The experimental performance and analytical performance predictions, along with design requirements for producing practical PL seals, result in the following conclusions:

1. Low modulus materials such as PTFE, although possessing limited high temperature capability and cold flow resistance, produced the best PL seal performance. This performance advantage is attributed to the inability of high modulus materials to conform to slight machining irregularities, resulting in excessive gas leakage. The high elastic modulus materials also require very small rod interferences if the seal is to be assembled. This means that seals must be manufactured to more precise tolerances, always difficult in plastic.

2. The ring-expanded inlet PL seal was shown to be an excellent oil pump. Predicted pumping rates, based on film thickness calculations, are in reasonable agreement.

3. The prediction of lower-than-experienced pumping rates is attributed to a lower prediction of velocity effects and the absence of squeeze-film behavior in the analysis. The squeeze-film analysis was not included in the present work since it is felt that a starved PL seal acting in a gas, oil-spray environment would exhibit little squeeze-film behavior.

Since PL seals are not contemplated to be used as oil pumps, the addition of squeeze-film behavior to the present analysis should not have a high priority. It can, however, have a beneficial effect on seal lubrication which should be considered. Of primary importance to seal development is the search for low modulus seal materials that do not exhibit cold flow from which better PL seals could be manufactured. With a wider selection of available materials, a statistically sound test program with a sufficent sample size should be initiated.

6.0 REFERENCES

1. Eusepi, M. W. et al. "Performance of Oil Pumping Rings: An Analytical and Experimental Study." MTI 86TR17, NASA CR-175083, January 1986.

2. Eusepi, M. W. et al. "Experimental Evaluation of Oil Pumping Rings." DOE/NASA/0119-81, NASA CR-165271, U.S. Department of Energy, April 1981.

APPENDIX

COMPUTER PROGRAM PLGRAD

Computer program PLGRAD, which has been used to generate performance data used in this report, is listed herein. The FORTRAN listing of program PLGRAD FORTRAN is preceded by an input description, an output description, and sample inputs and outputs. The sample input file and corresponding output file are for an unworn and worn phenylene oxide seal.

A.1 Input Description

The program uses namelist input. Definitions of the namelist quantities are given below.

Parameter No.	Namelist Name	Definition
1	DIMM	Seal ID (mm)
2	DSMM	Shaft Diameter (mm)
3	DOMM	Seal OD (mm)
4	STMM	Stroke (mm)
5	VICP	Viscosity (Cp)
6	EPSI	Elastic Modulus ($lb/in.^2$)
7	RPM	Speed (rpm)
8	RIMM	Radial Ring Interference (mm)
9	HPMP	External-Inlet Pressure (MPa)
10	POIS	Poisson's Ratio
	IWORN	0, Unworn or 1, Worn
	NP	Parameter No. to be Varied
	DX	Parameter Increments
	N	Number of Points

The program performs N calculations starting with the input value of parameter NP, then increments by DX, N-1 times.

A.2 Output Description

The outputs are in the form of a four-column table. The first column contains the parameters selected by the input value NP. The remaining columns are:

HMIC = Film Thickness (10^{-6} m)
PMPA = Interface Pressure (MPa)
CCPM = Flow Rate for Double-Acting Seal (cc/min)

A.3 Sample Input

```
&INPUTS
DIMM=18.850,     DSMM=19.00,     DOMM=22.00,     STMM=50.80,
VICP=55.,        EPSI=0.38E6,     RPM=1000.,     RIMM=.25,
HPMP=0.,         POIS=0.46,        IWORN=0,
  NP=7,            DX=100.,         N=10,
&END
&INPUTS IWORN=1,&END
```

A.4 Sample Output

RPM	HMIC	PMPA	CCPM
1.00000D+03	5.21409D+00	2.96753D+00	9.75272D+00
1.10000D+03	5.57180D+00	2.96753D+00	1.14640D+01
1.20000D+03	5.91862D+00	2.96753D+00	1.32846D+01
1.30000D+03	6.25562D+00	2.96753D+00	1.52111D+01
1.40000D+03	6.58372D+00	2.96753D+00	1.72404D+01
1.50000D+03	6.90366D+00	2.96753D+00	1.93695D+01
1.60000D+03	7.21609D+00	2.96753D+00	2.15958D+01
1.70000D+03	7.52160D+00	2.96753D+00	2.39170D+01
1.80000D+03	7.82067D+00	2.96753D+00	2.63308D+01
1.90000D+03	8.11374D+00	2.96753D+00	2.88351D+01

RPM	HMIC	PMPA	CCPM
1.00000D+03	5.96042D+00	2.96753D+00	1.11487D+01
1.10000D+03	6.55646D+00	2.96753D+00	1.34899D+01
1.20000D+03	7.15251D+00	2.96753D+00	1.60541D+01
1.30000D+03	7.74855D+00	2.96753D+00	1.88413D+01
1.40000D+03	8.34459D+00	2.96753D+00	2.18514D+01
1.50000D+03	8.94063D+00	2.96753D+00	2.50846D+01
1.60000D+03	9.53667D+00	2.96753D+00	2.85407D+01
1.70000D+03	1.01327D+01	2.96753D+00	3.22197D+01
1.80000D+03	1.07288D+01	2.96753D+00	3.61218D+01
1.90000D+03	1.13248D+01	2.96753D+00	4.02468D+01

A.5 PLGRAD FORTRAN Listing

```
C$ H2                                                                    PLG00010
C THIS IS THE DIMENSIONAL INLET PROGRAM.                                 PLG00020
      COMMON/BINP/DIMM,DSMM,DOMM,STMM,VICP,EPSI,RPM,SDEG,HPMP,POIS,DMMM  PLG00030
C HERE HPMP DENOTES DIFFERENCE BETWEEN EXTERNAL AND INLET PRESSURES.     PLG00040
      DIMENSION A(11)                                                    PLG00050
      EQUIVALENCE (A(1),DIMM)                                            PLG00060
      NAMELIST/INPUTS/DIMM,DSMM,DOMM,STMM,                               PLG00070
     +VICP,EPSI,RPM,RIMM,HPMP,POIS,DMMM,IWORN,NP,N,DX,IPAR               PLG00080
      INTEGER STR(11)/'DIMM','DSMM','DOMM','STMM','VICP','EPSI',         PLG00090
     +'RPM ','RIMM','HPMP','POIS','DMMM'/                               PLG00100
C     DATA ISL,IRI/'SDEG','RIMM'/,IRN/'RIMM'/                            PLG00110
      DATA IRN/'RIMM'/                                                   PLG00120
      PI=4.*ATAN(1.)                                                     PLG00130
      IPAR=0                                                             PLG00140
    1 READ(05,INPUTS,END=999)                                            PLG00150
      SDEG=RIMM                                                          PLG00160
      IRAD=2                                                             PLG00170
      IF(IWORN.NE.0)IRAD=3                                               PLG00180
      AINIT=A(NP)                                                        PLG00190
      A(NP)=A(NP)-DX                                                     PLG00200
      STR(8)=IRN                                                         PLG00210
C     IF(IRAD.EQ.1)STR(8)=IRI                                            PLG00220
      IF(IRAD.EQ.2)STR(8)=IRN                                            PLG00230
```

```
      IF(IRAD.EQ.3)STR(8)=IRN                                          PLG00240
      IF(IPAR.NE.1)PRINT 20,STR(NP)                                    PLG00250
   20 FORMAT(//8X,A4,11X,'HMIC',11X,'PMPA',11X,'CCPM'/)                PLG00260
      DO 5 I=1,N                                                       PLG00270
      A(NP)=A(NP)+DX                                                   PLG00280
      DI=A(1)*.001                                                     PLG00290
      DS=A(2)*.001                                                     PLG00300
      DO=A(3)*.001                                                     PLG00310
      ST=A(4)*.001                                                     PLG00320
      VI=A(5)*.001                                                     PLG00330
      E=A(6)*6895.                                                     PLG00340
      EN=A(7)/60.                                                      PLG00350
      SL=A(8)*PI/180.                                                  PLG00360
      RI=A(8)*.001                                                     PLG00370
      HP=A(9)*1.E6                                                     PLG00380
      PO=A(10)                                                         PLG00390
      DM=A(11)*.001                                                    PLG00400
      U=2.*EN*ST                                                       PLG00410
      T=(DO-DI)/2.                                                     PLG00420
      T2=(DM-DI)/2.                                                    PLG00430
      R=(DI+DO)/4.                                                     PLG00440
      DEL=(-DI+DS)/2.                                                  PLG00450
      RMX=(DI+DM)/4.                                                   PLG00460
      P0=DEL*E*T/R/R+HP                                                PLG00470
      P2=DEL*E*T2/RMX/RMX+HP                                           PLG00480
      DEL0=HP*R*R/E/T                                                  PLG00490
      DELT=DEL+DEL0                                                    PLG00500
      R2=SQRT(2.)                                                      PLG00510
      H0=3.*VI*U/P0/SL                                                 PLG00520
      DF=E*T**3/12./(1.-PO**2)                                         PLG00530
      ELDF=(R*R*DF/E/T)**.25                                           PLG00540
      BCON=6.*U*VI*ELDF*R*R/E/T                                        PLG00550
      BET1=BCON/(DELT)**3                                              PLG00560
      DBAR=(RI-DEL)/DELT                                               PLG00570
      THBAR=SL*ELDF/DELT                                               PLG00580
      THEBAR=THBAR-.200039                                             PLG00590
      THWBAR=THBAR-.5/R2                                               PLG00600
      FCON=DF/ELDF**3*DELT                                             PLG00610
      F1NPMM=2.49951*FCON*1.E-3                                        PLG00620
      F2NPMM=.42175*FCON*1.E-3                                         PLG00630
      ELF2MM=ELDF*1.6790*1.E3                                          PLG00640
      SEDEG=THEBAR*DELT/ELDF*180./PI                                   PLG00650
      IF(IRAD.NE.0)GO TO 222                                           PLG00660
      H1=H0*THBAR/THEBAR                                               PLG00670
      H0=(BCON/BETSL(BET1,SL,DELT/ELDF))**(1./3.)                      PLG00680
      PMMPA=P0*H1/H0*1.E-6                                             PLG00690
  222 IF(IRAD.EQ.1)H0=(6.*PI/16.*SQRT(2.*RI)*VI*U/P0)**(2./3.)         PLG00700
      IF(IRAD.NE.2)GO TO 90                                            PLG00710
      CALL BETCAL(BET1,DBAR,BETA,XM,PM)                                PLG00720
      H0=(BCON/BETA)**(1./3.)                                          PLG00730
      PMMPA=PM*P0*1.E-6                                                PLG00740
      STRMPA=RI*E/R*1.E-6                                              PLG00750
      XMMM=XM*ELDF*1000.                                               PLG00760
   90 IF(IRAD.NE.3)GO TO 60                                            PLG00770
```

```
      CALL RINSBW((RI+DELO)/DELT,WP,ELCN)                                PLG00780
      SLW=WP*DELT/ELDF                                                   PLG00790
      HO=3.*VI*U/PO/SLW                                                  PLG00800
   60 CONTINUE                                                           PLG00810
      IF(IRAD.EQ.4)HO=HO*THBAR/THWBAR                                    PLG00820
      Q=U*HO*(PI/2.)**3*DS/4.                                            PLG00830
      CCPM=Q*60.*1.E6                                                    PLG00840
      HMIC=HO*1.E6                                                       PLG00850
      PMPA=PO*1.E-6                                                      PLG00860
      P2MPA=P2*1.E-6                                                     PLG00870
      ELDFMM=ELDF*1000.                                                  PLG00880
      DELTMM=DELT*1000.                                                  PLG00890
      IF(IPAR.EQ.1)GO TO 61                                              PLG00900
      PRINT 21,A(NP),HMIC,PMPA,CCPM                                      PLG00910
      GO TO 5                                                            PLG00920
   61 BETA=6.*U*VI*ELDF/HO**3*R*R/E/T                                    PLG00930
      WRITE(6,1000)STR(NP),A(NP),CCPM,HMIC                               PLG00940
 1000 FORMAT(/1X,A4,'=',G15.7,5X,'CCPM=',G15.7,5X,'HMIC=',G15.7)         PLG00950
      WRITE(6,1200)PMPA,P2MPA,ELDFMM,BETA                                PLG00960
 1200 FORMAT(1X,'PMPA=',G15.7,5X,'P2MPA=',G15.7,5X,/1X,                  PLG00970
     +'ELDFMM=',G15.7,5X,'BETA=',G15.7)                                  PLG00980
      IF(IRAD.EQ.2.OR.IRAD.EQ.3)GO TO 888                                PLG00990
      GO TO 887                                                          PLG01000
  888 WRITE(6,1700)DELTMM,BET1,DBAR,STRMPA                               PLG01010
 1700 FORMAT(1X,'DELTMM=',G15.7,5X,'BET1=',G15.7,5X,                     PLG01020
     +'DBAR=',G15.7,5X,/1X,'STRMPA=',G15.7)                              PLG01030
      GO TO 886                                                          PLG01040
  887 WRITE(6,1400)DELTMM,BET1,THEBAR                                    PLG01050
 1400 FORMAT(1X,'DELTMM=',G15.7,5X,'BET1=',G15.7,5X,'THEBAR=',G15.7)     PLG01060
      WRITE(6,1600)F1NPMM,F2NPMM,ELF2MM,THBAR,THWBAR                     PLG01070
 1600 FORMAT(1X,'F1NPMM=',G15.7,5X,'F2NPMM=',G15.7,5X,/1X,               PLG01080
     +'ELF2MM=',G15.7,5X,'THBAR=',G15.7,5X,/1X,'THWBAR=',G15.7)          PLG01090
      IF(IRAD.EQ.0)WRITE(6,1500)SEDEG,PMMPA                              PLG01100
 1500 FORMAT(1X,'SEDEG=',G15.7,5X,'PMMPA=',G15.7)                        PLG01110
      GO TO 5                                                            PLG01120
  886 IF(IRAD.EQ.2)WRITE(6,1300)XMMM,PMMPA                               PLG01130
 1300 FORMAT(1X,'XMMM=',G15.7,5X,'PMMPA=',G15.7)                         PLG01140
    5 CONTINUE                                                           PLG01150
   21 FORMAT(1P4E15.5)                                                   PLG01160
      A(NP)=AINIT                                                        PLG01170
      GO TO 1                                                            PLG01180
  999 STOP                                                               PLG01190
      END                                                                PLG01200
      FUNCTION YLAG(XI,X,Y,IND,N1,IMAX,IEX)                              PLG01210
      DIMENSION X(1),Y(1)                                                PLG01220
      N=N1                                                               PLG01230
      IEX=0                                                              PLG01240
      IF(N.LE.IMAX) GO TO 1                                              PLG01250
      N=IMAX                                                             PLG01260
      IEX=N                                                              PLG01270
    1 IF(IND.GT.0) GO TO 4                                               PLG01280
      DO 2 J=1,IMAX                                                      PLG01290
      IF(XI-X(J))3,13,2                                                  PLG01300
    2 CONTINUE                                                           PLG01310
```

```
      IEX=1                                                              PLG01320
      GO TO 7                                                            PLG01330
    3 IND=J                                                              PLG01340
    4 CONTINUE                                                           PLG01350
      IF(IND.GT.1)GO TO 5                                                PLG01360
      IEX=-1                                                             PLG01370
    5 INL=IND-(N+1)/2                                                    PLG01380
      IF(INL.GT.0) GO TO 6                                               PLG01390
      INL=1                                                              PLG01400
    6 INU=INL+N-1                                                        PLG01410
      IF(INU.LE.IMAX) GO TO 8                                            PLG01420
    7 INL=IMAX-N+1                                                       PLG01430
      INU=IMAX                                                           PLG01440
    8 S=0.                                                               PLG01450
      DO 30 J=INL,INU                                                    PLG01460
      IF(XI.EQ.X(J)) GO TO 13                                            PLG01470
   30 CONTINUE                                                           PLG01480
      P=1.                                                               PLG01490
      DO 11 J=INL,INU                                                    PLG01500
      P=P*(XI-X(J))                                                      PLG01510
      D=1.                                                               PLG01520
      DO 10 I=INL,INU                                                    PLG01530
      IF(I.NE.J) GO TO 9                                                 PLG01540
      XD=XI                                                              PLG01550
      GO TO 10                                                           PLG01560
    9 XD=X(J)                                                            PLG01570
   10 D=D*(XD-X(I))                                                      PLG01580
   11 S=S+Y(J)/D                                                         PLG01590
      YLAG=S*P                                                           PLG01600
   12 RETURN                                                             PLG01610
   13 YLAG=Y(J)                                                          PLG01620
      GO TO 12                                                           PLG01630
      END                                                                PLG01640
      SUBROUTINE RINSBW(D,S,ELC)                                         PLG01650
      DIMENSION Z(33),RD(33),WP(33)                                      PLG01660
      DATA Z,RD,WP/                                                      PLG01670
     +0.0      ,0.100000,0.200000,0.300000,0.400000,0.500000,0.600000,   PLG01680
     +0.700000,0.800000,0.900000,1.000000,1.100000,1.200000,1.300000,   PLG01690
     +1.400000,1.500000,1.600000,1.700000,1.800000,1.900000,2.000000,   PLG01700
     +2.100000,2.200000,2.300000,2.400000,2.500000,2.600000,2.700000,   PLG01710
     +2.800000,2.900000,3.000000,3.100000,3.200000,                     PLG01720
     +0.0      ,0.058137,0.113905,0.167663,0.219709,0.270295,0.319644,   PLG01730
     +0.367955,0.415412,0.462189,0.508452,0.554369,0.600107,0.645841,   PLG01740
     +0.691754,0.738045,0.784933,0.832661,0.881509,0.931801,0.983925,   PLG01750
     +1.038346,1.095644,1.156553,1.222030,1.293364,1.372356,1.461642,   PLG01760
     +1.565312,1.690222,1.849200,2.070620,2.439467,                     PLG01770
     +0.0      ,0.052582,0.100776,0.145235,0.186492,0.224989,0.261100,   PLG01780
     +0.295148,0.327413,0.358145,0.387572,0.415899,0.443322,0.470026,   PLG01790
     +0.496192,0.521999,0.547635,0.573295,0.599191,0.625562,0.652681,   PLG01800
     +0.680876,0.710548,0.742207,0.776520,0.814399,0.857135,0.906661,   PLG01810
     +0.966037,1.040530,1.140267,1.288397,1.557204/                     PLG01820
      XI=SQRT(SQRT(ABS(D-1.)))                                           PLG01830
      IND=0                                                              PLG01840
      S=YLAG(XI,RD,WP,IND,3,33,IEX)**3                                   PLG01850
```

```
      ELC=YLAG(XI,RD,Z,IND,3,33,IEX)                                    PLG01860
      RETURN                                                            PLG01870
      END                                                               PLG01880
      SUBROUTINE BETCAL(BET1,DBAR,BETA,XM,PM)                           PLG01890
      DIMENSION HL1(13),CL(13)                                          PLG01900
      DIMENSION HL(7),WK1(30),HLP(1),BLP(1),ANS(1,7)                    PLG01910
      DIMENSION BQ(8),AQ(8,7)                                           PLG01920
      DIMENSION BL(11),PMAX(11,7),XPM(11,7)                             PLG01930
      DATA HL1,CL/                                                      PLG01940
     +-0.69315,-0.35667, 0.0,     0.40547, 0.69315, 1.09861, 1.60944,   PLG01950
     + 1.94591, 2.30258, 2.70805, 2.99573, 3.40120, 3.91202,            PLG01960
     + 0.33611, 0.61215, 0.91745, 1.28623, 1.56603, 1.99386, 2.60543,   PLG01970
     + 3.06409, 3.60775, 4.30551, 4.85468, 5.70445, 6.89099/            PLG01980
      DATA HL/                                                          PLG01990
     +-0.69315, 0.0    , 0.69315, 1.60944, 2.30258, 2.99573, 3.91202/   PLG02000
      DATA BQ,AQ/                                                       PLG02010
     +3.68888,4.60517,5.29832,6.21461,6.90776,7.60090,8.51719,9.21034,  PLG02020
     +1.3849,1.1936,1.1249,1.0732,1.0491,1.0314,1.0152,1.0068,1.4179,   PLG02030
     +1.2394,1.1603,1.0927,1.0590,1.0355,1.0149,1.0055,1.5028,1.2931,   PLG02040
     +1.1937,1.1080,1.0660,1.0373,1.0134,1.0032,1.6240,1.3592,1.2331,   PLG02050
     +1.1257,1.0743,1.0395,1.0120,1.0009,1.7075,1.4036,1.2599,1.1381,   PLG02060
     +1.0801,1.0418,1.0117,0.9999,1.7801,1.4427,1.2836,1.1500,1.0865,   PLG02070
     +1.0448,1.0123,0.9996,1.8471,1.4800,1.3078,1.1625,1.0938,1.0488,   PLG02080
     +1.0137,1.0000/                                                    PLG02090
      DATA BL/                                                          PLG02100
     + 3.91202, 4.60517, 5.29832, 6.21461, 6.90776, 7.60090, 8.51719,   PLG02110
     + 9.21034, 9.90349,10.81978,11.51293/                              PLG02120
      DATA PMAX/                                                        PLG02130
     + 1.2663, 1.2920, 1.3492, 1.4653, 1.5830, 1.7270, 1.9613, 2.1767,  PLG02140
     + 2.4253, 2.8203, 3.1712, 1.4032, 1.4431, 1.5195, 1.6693, 1.8180,  PLG02150
     + 1.9986, 2.2902, 2.5608, 2.8624, 3.3510, 3.7765, 1.6138, 1.6687,  PLG02160
     + 1.7697, 1.9626, 2.1535, 2.3805, 2.7513, 3.0770, 3.4665, 4.0823,  PLG02170
     + 4.6141, 2.1068, 2.1874, 2.3331, 2.6122, 2.8847, 3.2108, 3.7360,  PLG02180
     + 4.2083, 4.7692, 5.6693, 6.4055, 2.8103, 2.9186, 3.1212, 3.5100,  PLG02190
     + 3.8943, 4.3533, 5.0870, 5.7528, 6.5590, 7.8223, 8.8493, 4.1202,  PLG02200
     + 4.2702, 4.5762, 5.1638, 5.7422, 6.4402, 7.5485, 8.5707, 9.7297,  PLG02210
     +11.5566,13.2670, 7.8978, 8.1913, 8.7706, 9.8989,11.0704,12.4201,  PLG02220
     +14.6704,16.6809,18.8944,22.5296,26.0613/                          PLG02230
      DATA XPM/                                                         PLG02240
     + 2.6129, 2.5787, 2.5384, 2.5012, 2.4752, 2.4525, 2.4348, 2.4167,  PLG02250
     + 2.4142, 2.4005, 2.3982, 2.9130, 2.8913, 2.8712, 2.8453, 2.8302,  PLG02260
     + 2.8176, 2.7979, 2.7795, 2.7871, 2.7741, 2.7736, 3.2143, 3.2114,  PLG02270
     + 3.2032, 3.1997, 3.1854, 3.1827, 3.1655, 3.1750, 3.1661, 3.1533,  PLG02280
     + 3.1584, 3.5742, 3.5968, 3.6157, 3.6279, 3.6292, 3.6356, 3.6362,  PLG02290
     + 3.6340, 3.6235, 3.6143, 3.6230, 3.7900, 3.8330, 3.8608, 3.8867,  PLG02300
     + 3.8989, 3.9033, 3.9084, 3.9093, 3.8992, 3.8893, 3.9040, 3.9448,  PLG02310
     + 4.0000, 4.0389, 4.0704, 4.0878, 4.0938, 4.1040, 4.1079, 4.1232,  PLG02320
     + 4.1263, 4.1069, 4.0669, 4.1267, 4.1738, 4.2214, 4.2349, 4.2593,  PLG02330
     + 4.2588, 4.2650, 4.2862, 4.2913, 4.2700/                          PLG02340
      HLP(1)=ALOG(DBAR)                                                 PLG02350
      IND=0                                                             PLG02360
      CON=EXP(YLAG(HLP(1),HL1,CL,IND,3,13,IEX))                         PLG02370
      BETAC=(CON/BET1)**(1./.8195)                                      PLG02380
      BETA=BETAC                                                        PLG02390
```

```
      IF(BETA.GT.1.E4)GO TO 5                                          PLG02400
      BLP(1)=ALOG(BETAC)                                               PLG02410
      CALL IBCIEU(AQ,8,BQ,8,HL,7,BLP,1,HLP,1,ANS,1,WK1,IER)            PLG02420
      BETA=ANS(1,1)*BETAC                                              PLG02430
    5 BLP(1)=ALOG(BETA)                                                PLG02440
      CALL IBCIEU(PMAX,11,BL,11,HL,7,BLP,1,HLP,1,ANS,1,WK1,IER)        PLG02450
      PM=ANS(1,1)                                                      PLG02460
      CALL IBCIEU(XPM,11,BL,11,HL,7,BLP,1,HLP,1,ANS,1,WK1,IER)         PLG02470
      XM=ANS(1,1)                                                      PLG02480
      RETURN                                                           PLG02490
      END                                                              PLG02500
      FUNCTION BETSL(BET1,SL,DOL)                                      PLG02510
      DIMENSION BL(13),BFN(13)                                         PLG02520
      DATA BL/                                                         PLG02530
     +13.12236,12.20607,11.51293,10.81978, 9.90349, 9.21034, 8.51719,  PLG02540
     + 7.60090, 6.90776, 6.21461, 5.29832, 4.60517, 3.91202/           PLG02550
      DATA BFN/                                                        PLG02560
     +-2.42400,-2.27362,-2.15682,-2.03710,-1.87397,-1.74656,-1.61545,  PLG02570
     +-1.43609,-1.29564,-1.15098,-0.95330,-0.79907,-0.64119/           PLG02580
      PAR=ALOG(.5*BET1**(2./3.)*DOL/(SL-DOL/SQRT(2.)))                 PLG02590
      IND=0                                                            PLG02600
      BETSL=EXP(YLAG(PAR,BFN,BL,IND,3,13,IEX))                         PLG02610
      RETURN                                                           PLG02620
      END                                                              PLG02630
```

ACKNOWLEDGMENT

The work reported in this document was performed by Mechanical Technology Incorporated (MTI), 968 Albany-Shaker Road, Latham, New York 12110, as prime contractor to the National Aeronautics and Space Administration's Lewis Research Center, Cleveland, Ohio 44135, under Prime Contract No. DEN3-343. The program is funded by the U.S. Department of Energy.

1. Report No.	2. Government Accession No.	3. Recipient's Catalog No.
NASA CR-179570		

4. Title and Subtitle	5. Report Date
EHD Analysis of and Experiments on Pumping Leningrader Seals	June 1986
	6. Performing Organization Code
7. Author(s)	8. Performing Organization Report No.
M.W. Eusepi and J.A. Walowit	MTI 86TR33
	10. Work Unit No.
9. Performing Organization Name and Address	11. Contract or Grant No.
Mechanical Technology Incorporated 968 Albany-Shaker Road Latham, New York 12110	DEN 3-343
	13. Type of Report and Period Covered
12. Sponsoring Agency Name and Address	Contractor Report
U.S. Department of Energy Office of Vehicle and Engine R&D Washington, D.C. 20545	14. Sponsoring Agency ~~Code~~ Report No. DOE/NASA/0343-1

15. Supplementary Notes

Final Report. Prepared under Interagency Agreement DE-AI01-85CE50112. Project Manager, W. Tomazic, Power Technology Division, NASA Lewis Research Center, Cleveland, Ohio 44135.

16. Abstract

Analysis and design charts have been generated to provide design data for Pumping Leningrader Reciprocating Rod Seals. The analytical treatment divides the seal into three regions: an inlet zone, induced with the use of an expansion ring, a contact zone, and an exit zone. Complete solutions have been obtained by matching elasticity equations with hydrodynamic theory. Experiments, although of a limited nature, did demonstrate the ability of the seal design analysis to provide viable seals.

17. Key Words (Suggested by Author(s))	18. Distribution Statement
Pumping Leningrader seal Reciprocating rod seal analysis Stirling engine piston rod seal Reciprocating rod seal design	Unclassified - unlimited STAR Category 37 DOE Category UC-96

19. Security Classif. (of this report)	20. Security Classif. (of this page)	21. No. of pages	22. Price*
Unclassified	Unclassified	90	A05

*For sale by the National Technical Information Service, Springfield, Virginia 22161